

Article

Not peer-reviewed version

---

# Growth Light Quality Influences the Temperature of the Leaf Surface via Regulation of the Rate of NPQ Thermal Dissipation and Stomatal Conductance

---

[Magdalena Trojak](#) \* and [Ernest Skowron](#)

Posted Date: 18 October 2023

doi: [10.20944/preprints202310.1103.v1](https://doi.org/10.20944/preprints202310.1103.v1)

Keywords: leaf surface temperature; thermal imaging; chlorophyll fluorescence quenching; indoor farming; light quality; LED; non-photochemical quenching; FLIR



Preprints.org is a free multidiscipline platform providing preprint service that is dedicated to making early versions of research outputs permanently available and citable. Preprints posted at Preprints.org appear in Web of Science, Crossref, Google Scholar, Scilit, Europe PMC.

Copyright: This is an open access article distributed under the Creative Commons Attribution License which permits unrestricted use, distribution, and reproduction in any medium, provided the original work is properly cited.

Disclaimer/Publisher's Note: The statements, opinions, and data contained in all publications are solely those of the individual author(s) and contributor(s) and not of MDPI and/or the editor(s). MDPI and/or the editor(s) disclaim responsibility for any injury to people or property resulting from any ideas, methods, instructions, or products referred to in the content.

## Article

# Growth Light Quality Influences the Temperature of the Leaf Surface via Regulation of the Rate of NPQ Thermal Dissipation and Stomatal Conductance

Magdalena Trojak <sup>1,\*</sup> and Ernest Skowron <sup>2</sup>

<sup>1</sup> Department of Environmental Biology, Jan Kochanowski University, Uniwersytecka 7, 25-406 Kielce, Poland

<sup>2</sup> Department of Environmental Biology, Jan Kochanowski University, Uniwersytecka 7, 25-406 Kielce, Poland; ernest.skowron@ujk.edu.pl

\* Correspondence: magdalena.trojak@ujk.edu.pl; Tel.: +48-41-3496356

**Abstract:** Lots of efforts are made to optimize spectrum quality used for indoor farming to maximize artificial light utilization and reduce water loss. For such an improvement, green (G) light supplementation to a red-blue (RB) background was successfully employed in our previous studies to restrict both non-photochemical thermal dissipation (NPQ) and stomatal conductance ( $g_s$ ). At the same time, however, the downregulation of NPQ and  $g_s$  influences the leaf temperature ( $T_{leaf}$ ) in opposite ways. Thus, to elucidate which factor plays a more prominent role in  $T_{leaf}$  regulation and whether such response is temporal or permanent we investigated the correlation between NPQ or  $g_s$  and the subsequent  $T_{leaf}$ . To this end, we analysed tomato plants (*Solanum lycopersicum* L. cv. Malinowy Ozarowski) grown solely under monochromatic LED lamps (435, 520, or 662 nm; 80  $\mu\text{mol m}^{-2} \text{s}^{-1}$ ) or under mixed RGB spectrum (1:1:1; 180  $\mu\text{mol m}^{-2} \text{s}^{-1}$ ), and simultaneously measured the  $g_s$  and  $T_{leaf}$  with an infrared gas analyser and thermocouple or employed infrared thermal camera (FLIR) during thermal imaging analyses. Results documented that growth light quality significantly modified the  $T_{leaf}$ , and such response is not temporal. Furthermore, we found that plants' actual adaxial leaf surface temperature is more closely related to NPQ amplitude, while the temperature of the abaxial surface corresponds to  $g_s$ .

**Keywords:** leaf surface temperature; thermal imaging; chlorophyll fluorescence quenching; indoor farming; light quality; LED; non-photochemical quenching; FLIR

## 1. Introduction

Plants, as sessile organisms, have evolved different defence responses to encounter environmental stresses such as drought, suboptimal temperature, and light stress. Activated regulatory mechanisms might however overlap in not obvious way affecting plant physiology. As an example, the non-photochemical thermal dissipation and stomatal conductance regulation might be considered. Stomatal conductance ( $g_s$ ) is a major regulator of carbon dioxide and water vapour exchange between the leaf interior and the surrounding atmosphere [1]. Thus, the rate of  $g_s$  is related to crop yield and its regulation needs to fulfil opposite roles of minimizing water loss, and at the same time sustaining effective  $\text{CO}_2$  influx. Yet, the restriction of leaf  $g_s$  regulated by chemical and/or hydraulic signals affects the rate of transpiration ( $E$ ) and consequently the leaf surface temperature ( $T_{leaf}$ ) [2]. Also, the meaning of the thermal dissipation process, called non-photochemical quenching (NPQ), which is crucial to minimize the risk of potential damage, is complex. On the one hand, the induction of NPQ acts as a safety valve allowing to dissipate excess light energy absorbed with photosynthetic pigments in the form of harmless heat [3]. On the other, however, whilst the induction of NPQ is rapid, its relaxation is a prolonged process limiting the photosynthesis, even despite the fact light intensity might already shift towards optimal dose [4]. Furthermore, as the up- or downregulation of both processes, i.e.,  $g_s$  and NPQ influences  $T_{leaf}$  in opposite ways, more attention

should be paid to elucidate which factor plays a more prominent role in its regulation. NPQ includes components with different mechanisms and characteristic times, such as energy-dependent ( $qE$ ), zeaxanthin (Z)-dependent ( $qZ$ ), photoinhibitory ( $qI$ ), or state transition-related ( $qT$ ) [5]. However, considering the aims of the study we focus on the  $qZ$  because the accumulation of Z facilitates the dissipation of excess energy via heat [6].

Previous research concluded that relationships between  $g_s$  and NPQ-generated heat are tight almost exclusively under strong actinic light [7]. Other papers [8] also proved a positive non-linear correlation with the extent of NPQ induction resulting in higher leaf temperatures in response to increasing illumination. Another study [9] stated that despite the existence of a positive relationship between NPQ and leaf temperature change ( $\Delta T_{leaf}$ ), the strength of its coupling varies. The authors concluded that enhanced heat exchange managed with NPQ induction might be latent due to additional uncontrolled heat dissipation or closure of stomata.

Furthermore, the current understanding of light-driven modification of leaf temperature is restricted to analyses concerning changes in incident light intensity [10]. In such cases, when plants are grown under a unified light quality, the actual foliar temperature measured under changing light intensity is primarily related to the stomatal aperture regulation rather than NPQ amplitude [11]. However, it is still unclear how the different light quality affects  $T_{leaf}$ . Such a response, however, might be highly expected as in previous studies [3,12] we documented that stomatal conductance as well as NPQ are related to lighting spectra applied during plant growth in controlled environment agriculture. It has been noticed that progressive replacement of R light by G light in the growth RB spectrum contracts stomatal dimension, thus reducing  $g_s$  and  $E$ , and consequently improving water-use efficiency [12], but decreasing, at the same time, the evaporative cooling and presumably increasing the foliar temperature [11]. Also, little is known about the direct effect of  $T_{leaf}$  on  $g_s$ , which may exist independently from effects exerted through changes in plant water status [13].

Moreover, examined NPQ value in tomato plants grown under monochromatic (R, G or B) or mixed RGB (1:1:1) light confirmed that R- and B-light treatments enhanced the NPQ amplitude while the plants grown under G and RGB spectrum presented a significantly lower amplitude of NPQ due to the reduced accumulation of NPQ-related proteins (PsbS, VDE, cyt f and PGRL1) [3]. Also, another study [14] documented that NPQ amplitude is increased in tomato plants grown under RB- and monochromatic B-light spectrum compared to values noted under white light with G-light (544 nm) peak wavelength.

Altogether, the above results prompted questions regarding the role of the spectrum in determining leaf temperature. Firstly, the intriguing question is whether the application of monochromatic G light for plant cultivation or its introduction to the RB spectrum increases the actual  $T_{leaf}$  due to reduced  $g_s$  or decreases it due to restricted induction and amplitude of NPQ. It might be also presumed that the mentioned effects exerted by specific light simply cancel each other. Secondly, we asked if we would be able to notice differences in  $T_{leaf}$  related to the previous growth spectrum as a temporal or permanent phenomenon. In the first case, it could be explained by the redox state change or chloroplast inner membranes reorganization and/or light-driven stomatal movement, thus such a response might be omitted with previous analyses. Whilst the permanent phenomenon should be rather addressed to different patterns of gene expression and protein accumulation and/or modified leaf anatomy, it would be easier to notice, as it does not expire quickly during measurements when plants are exposed to certain actinic light or dark acclimation. Thus, the underlying concept of the present study is to elucidate the influence of spectrum-related thermal dissipation and stomatal conductance regulation on actual foliar temperature leading to differences in evaporation and consequently water use efficiency in plants grown under different light regimes. Furthermore, as associated fluctuations in  $T_{leaf}$  under different light regimes are expected to influence photosynthesis directly because it is a highly temperature-dependent process [10], we also analysed the photosynthetic activity of plants.

To this end, we employed different independent experiments with tomato plants grown under certain light regimes. First, we measured the  $T_{leaf}$  directly in growth chambers with a forward-looking infrared (FLIR) camera and analysed stomatal traits in the tomato plants. Then, we simultaneously

measured the  $g_s$  and temperature of the stomata-rich abaxial leaf surface within an infrared gas analyser (IRGA) and calibrated thermocouple placed inside the transparent gas exchange cuvette, as described previously [15], illuminated with RGB light composition at constant intensity. Next, we analysed gas exchange parameters also within IRGA, but in response to increasing light intensity. Then, based on methods described earlier [7,16] we conducted analyses of chlorophyll fluorescence imaging with a PAM fluorometer, monitoring NPQ amplitude with increasing light intensity (RLC, rapid light curve), and concurrent analysis of adaxial (illuminated) leaf surface temperature with FLIR camera. Also, to distinguish between NPQ- and  $g_s$ -related  $T_{leaf}$  change during RLC, we applied dithiothreitol (DTT) as a potent inhibitor of qZ component rise, thus significantly lowering the NPQ [3]. Then we plotted a model curve of the received results of  $\Delta NPQ/\Delta NPQ_{DTT}$  or  $\Delta g_s$  against  $\Delta T_{leaf}$  and assessed the data fitting. This study provides valuable information about imaging methodologies such as FLIR and PAM suitable to predict plant response to different light compositions within relevant traits such as the rate of evaporation, photochemical light utilization, and leaf temperature.

## 2. Results

### 2.1. Influence of grow light spectra on the energy quenching and adaxial leaf surface temperature

The effect of different growth light quality (Figure 1) on adaxial surface temperature of 28 DAT (days after transplanting) tomato plants (*Solanum lycopersicum* L. cv. Malinowy Ozarowski) leaves was measured with forward-looking infrared (FLIR) camera (FLIR E50) under the chamber-specific light composition and air temperature of  $22 \pm 1$  °C. We observed no significant differences in adaxial foliar temperature between plants grown under combined RGB spectrum compared to G or B groups, despite the higher PAR in RGB chamber than those of G or B one ( $180 \mu\text{mol m}^{-2} \text{s}^{-1}$  versus  $80 \mu\text{mol m}^{-2} \text{s}^{-1}$ ) (Figure 2). Furthermore, approximately 5% higher foliar temperature was noted under the R LEDs emitting photons of lower energy and longer wavelength than those of G and B LEDs. Thus, similarly to previous research [11], our results proved that under low light intensity ( $\leq 180 \mu\text{mol m}^{-2} \text{s}^{-1}$ ) the differences in light quality have minor importance in the regulation of foliar temperature of the adaxial side.

However, as we previously documented [3,12] that light quality influences NPQ amplitude and stomatal conductance under higher PAR, we also decided to elucidate plants' response to such conditions and additionally monitored the temperature of the abaxial side of the leaf. To overcome the possible limitation of Z synthesis during NPQ formation, plants of all groups were exposed to 30 min pre-illumination with RGB light ( $400 \mu\text{mol m}^{-2} \text{s}^{-1}$ ) to activate de-epoxidation of violaxanthin (V) with violaxanthin de-epoxidase enzyme (VDE), which results in the accumulation of Z [17]. To inhibit VDE the part of the leaves was infiltrated with DTT, as the linear relationship between the rate of radiationless energy dissipation (heat dissipation) and Z content was previously noted [18,19]. To assess the influence of DTT on stomatal conductance [20] DTT-treated leaves were also analysed during gas exchange measurements.

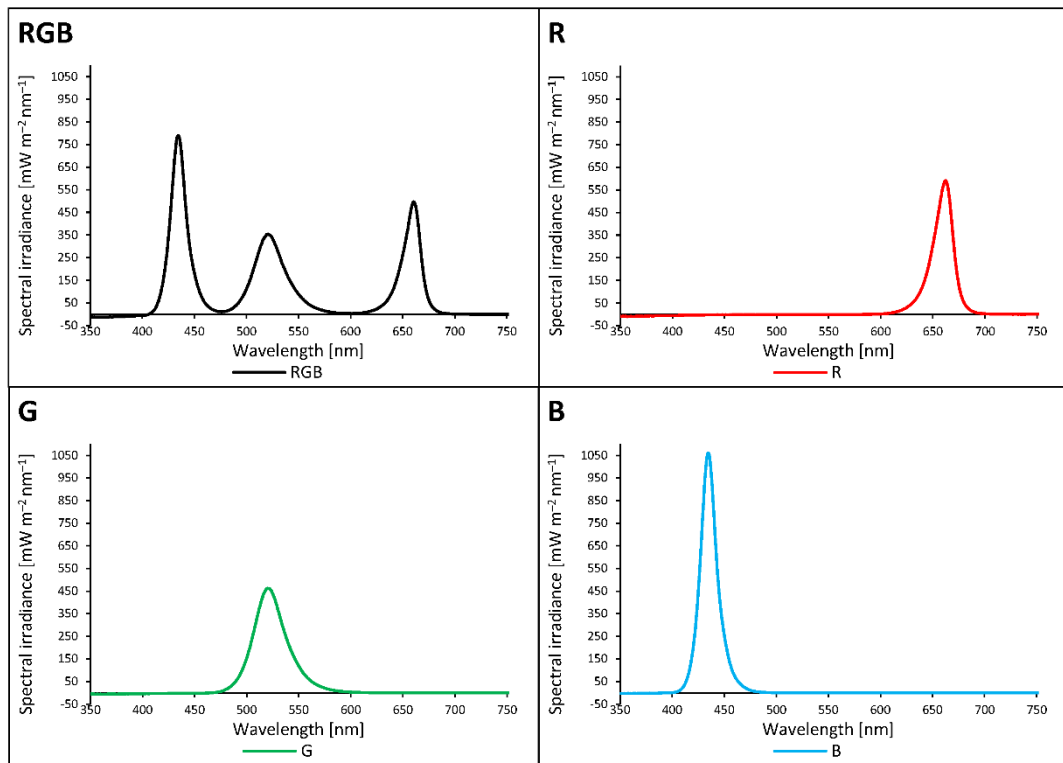


**Figure 1.** The light spectra of growth chambers were recorded with a spectroradiometer at six locations at the level of the apical bud and averaged. Plants of RGB (red-green-blue) chamber were grown under  $180 \mu\text{mol m}^{-2} \text{s}^{-1}$ , while R, G, and B groups were grown under  $80 \mu\text{mol m}^{-2} \text{s}^{-1}$ . RGB states for the control plants (R:G:B = 1:1:1). The rest of the plants were grown solely under the monochromatic component of RGB spectrum each, provided by LED RhenacM12 lamps (PXM).

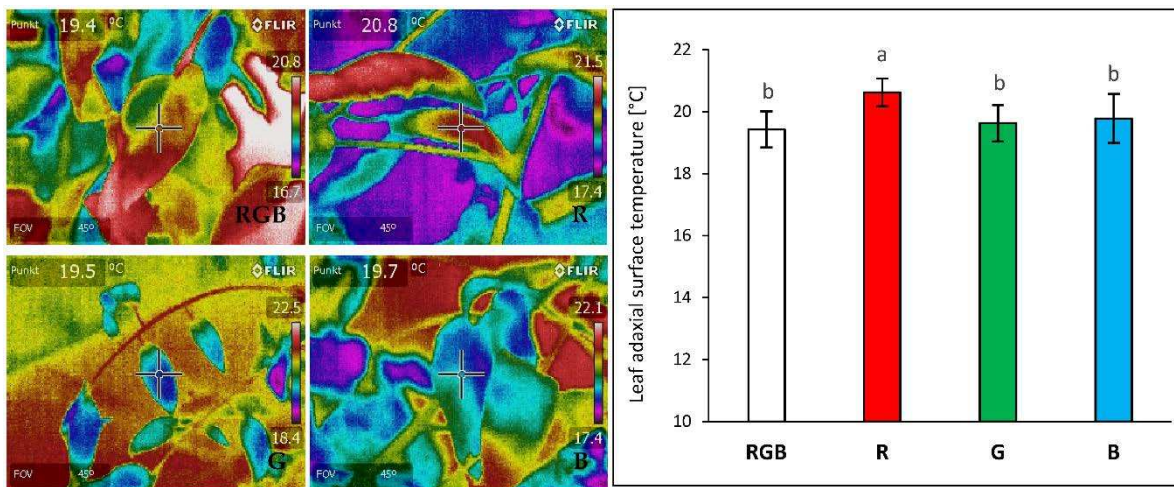


**Figure 2.** Effect of growth light quality on adaxial surface temperature of 28 DAT tomato plants (*Solanum lycopersicum* L. cv. Malinowy Ozarowski) leaves, measured with forward-looking infrared (FLIR) camera (FLIR E50) under the chamber-specific light and air temperature ( $22 \pm 1^\circ\text{C}$ ) conditions (see Material and Methods for details). The distance from the thermal camera to the leaf surface was approximately 0.3 m. Each bar represents the average  $\pm$  SD of six independent measurements ( $n = 6$ ). Different letters (a, b) indicate significant differences between treatments at  $p = 0.05$  with a Tukey's HSD test.

It has been documented that for unstressed leaves, the Fv/Fm value is highly consistent and oscillates at about 0.83 value, correlating to the maximum yield of photosynthesis [21]. Analysed data

of Fv/Fm share a general tendency noted in previous research [3], as the highest value of Fv/Fm of the water-treated sample was presented by plants grown under monochromatic blue light (Fv/Fm = 0.745) and the lowest under red (Fv/Fm = 0.547) and green one (Fv/Fm = 0.599) (Figure 3). At the same time, under RGB mixed spectrum we observed Fv/Fm = 0.717, which confirmed the postulated positive influence of B light on PSII vitality. We noted that DTT infiltration decreased Fv/Fm by about 14, 3 and 3% for RGB, G and B light, respectively, while in plants grown solely under R light, DTT treatment exerted a positive influence on Fv/Fm (+14%). The observed effect of DTT infiltration was more pronounced compared to previous research due to the enhanced infiltration period (60 min versus 30 min) and application of whole leaf immersed with petioles in a DTT-filled tube instead of leaf disc floating on DTT solution. Nonetheless, observed Fv/Fm values, in all treatments, were lower than expected indicating stressful conditions. A likely explanation is that leaf samples of plants grown under low PAR were subsequently exposed to higher light intensity during ChlF measurements, thus lowering the Fv/Fm value.

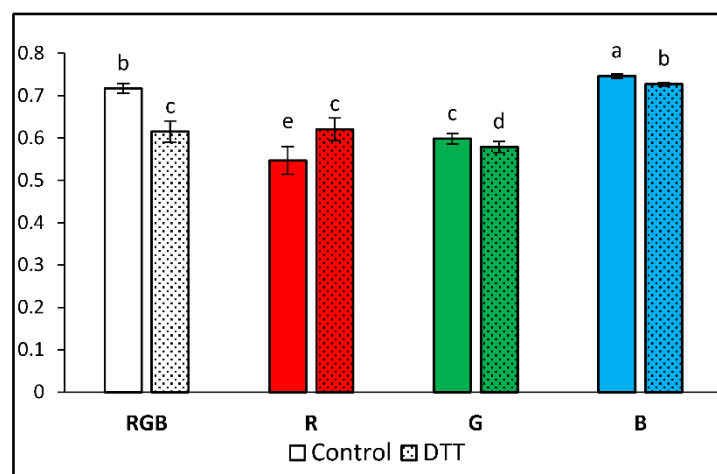


**Figure 3.** The maximal photochemical yield of PSII, Fv/Fm, in water- (control) or 5 mM DTT-infiltrated (DTT) leaves of 28 DAT tomato plants (*Solanum lycopersicum* L. cv. Malinowy Ozarowski) grown under different light conditions (see Material and Methods for details). Detached leaves were infiltrated for 1 h in the dark, followed by pre-illumination at  $400 \mu\text{mol m}^{-2} \text{s}^{-1}$  of RGB light for the next 30 min. The minimal fluorescence level (Fo) was measured by measuring modulated blue light (450 nm,  $0.01 \mu\text{mol m}^{-2} \text{s}^{-1}$ ). The maximal fluorescence level (Fm) was determined by a 0.8 s saturating blue light pulse (SP = 450 nm,  $5000 \mu\text{mol m}^{-2} \text{s}^{-1}$ ). Each bar represents the average  $\pm$  SD of six independent measurements ( $n = 6$ ). Different letters (a–e) indicate significant differences between the treatments at  $p = 0.05$  with a Tukey's HSD test.

We also analysed the induction of NPQ during RLC assay at increasing light intensity ( $0$ – $1250 \mu\text{mol m}^{-2} \text{s}^{-1}$ ) with simultaneous thermal imaging of  $T_{\text{adaxial}}$  at plateau phase of NPQ induction at  $396 \mu\text{mol m}^{-2} \text{s}^{-1}$  of water- (Figure 4a) and DTT-infiltrated leaves (Figure 4b). Analysed NPQ kinetics revealed a significant difference in maximal amplitude between groups both at plateau PAR as well as at PAR endpoint ( $1250 \mu\text{mol m}^{-2} \text{s}^{-1}$ ). In water-treated samples the highest NPQ level was observed in B and R plants, reaching 1.0 and about 0.75 (at  $396 \mu\text{mol m}^{-2} \text{s}^{-1}$ ), respectively, whereas in RGB and G groups at the plateau level, NPQ reaches 0.57 and 0.33. Moreover, the corresponding abaxial surface temperature reached 31.5, 29.2, 28.7 and 27.1 °C in B, R, RGB and G light-grown plants, respectively. As expected, in the case of leaves infiltrated with DTT we noted significantly reduced amplitude of NPQ compared to water control by 72, 60, 42 and 50% in RGB, R, G and B plants, respectively, whereas corresponding  $T_{\text{adaxial}}$  decreased by approximately 7, 6, 1 and 6% in B, R, G and RGB plants, respectively.

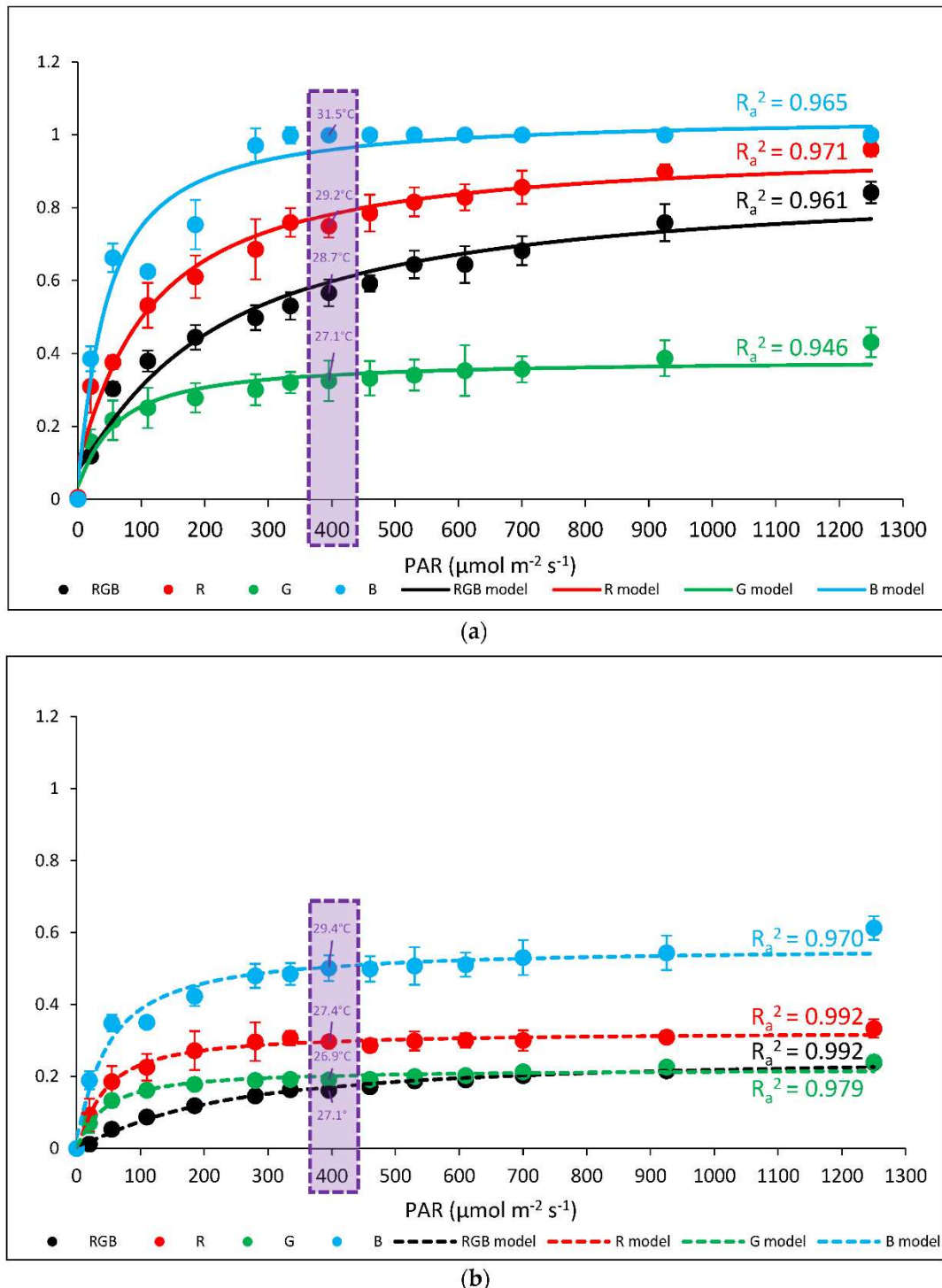


**Figure 4.** The non-photochemical quenching, NPQ, in water- (control; **a**) or 5 mM DTT-infiltrated (DTT, **b**) leaves of 28 DAT tomato plants (*Solanum lycopersicum* L. cv. Malinowy Ozarowski) grown under different light conditions (see Material and Methods for details). Detached leaves were infiltrated for 1 h in the dark, followed by pre-illumination at  $400 \mu\text{mol m}^{-2} \text{s}^{-1}$  of RGB light for the next 30 min. The dynamics of the NPQ were determined in re-darkened (30 min) leaf samples illuminated for 5 min at the following steps: 0, 20, 55, 110, 185, 280, 335, 395, 460, 530, 610, 700, 925 and  $1250 \mu\text{mol m}^{-2} \text{s}^{-1}$  of blue actinic light (AL = 450 nm) and saturating blue light pulse (SP = 450 nm,  $5000 \mu\text{mol m}^{-2} \text{s}^{-1}$ , duration 0.8 s) applied every 20 s at given AL intensity. Each data point represents the average  $\pm$  SD of six independent measurements ( $n = 6$ ; black = RGB, red = R, green = G, blue = B chamber). The inverse exponential regression model (Exp3P1Md) was employed to fit the experimental data. Fitting was applied as specified in Material and Methods and reported with an

adjusted  $R^2$  ( $R_a^2$ ) value to determine the goodness of data fitting. Adaxial surface temperature of leaves (dotted frame) was recorded simultaneously during chlorophyll fluorescence imaging (at  $25 \pm 1$  °C) after the NPQ parameter reached a plateau phase of induction at  $396 \mu\text{mol m}^{-2} \text{s}^{-1}$  with forward-looking infrared (FLIR) camera (FLIR E50, distance 0.3 m).

It should be, however, noted that ChlF analyses were performed at 25 °C, therefore to estimate the proper relationship between qZ NPQ induction and concomitant foliar temperature change during RLC we plotted  $\Delta\text{NPQ}$  against  $\Delta T_{\text{adaxial}}$ , assessed by subtracting values of NPQ values or adaxial leaf surface temperature (FLIR) estimated for control and DTT-infiltrated leaves at the same point of light intensity and quality ( $396 \mu\text{mol m}^{-2} \text{s}^{-1}$ , 450 nm) (Figure 5). Results showed a clear correlation between inhibition of DTT-sensitive NPQ component and restriction of temperature change of upper leaf side with both linear fitting model as well as non-linear Bradley model presented with 95% confidence band. Both functions present satisfactorily high goodness of data fitting with adjusted  $R^2$  of 0.997 and 0.996, respectively. We tested linear and non-linear regression model as previous research [11] postulated that at lower light intensities this relationship is non-linear and become linear at higher light intensities. The highest foliar temperature of the upper side accompanied by an induction of qZ-dependent heat dissipation was noted for plants previously grown under monochromatic B light, then the R and RGB plants, while the lowest values were recorded for G light-grown plants. The data obtained for all groups produced linear functions. Thus, results proved the existence of a relationship between heat dissipation through qZ induction and an increase of foliar temperature of adaxial, illuminated leaf side at higher PAR. Furthermore, as expected we documented differences in NPQ amplitude and  $T_{\text{adaxial}}$  as a result of previous growth light conditions and noticed that such a response is rather a permanent feature and did not expire after pre-illumination and dark adaptation.

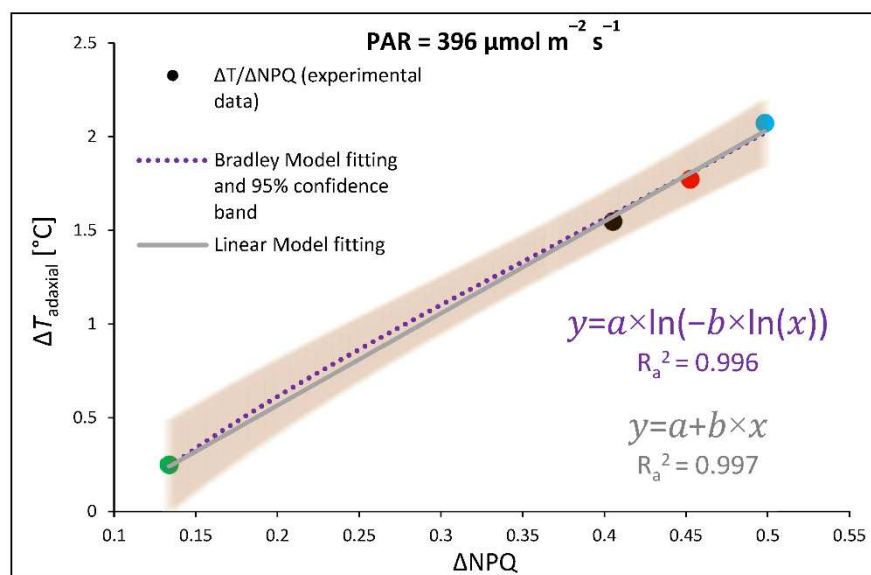


**Figure 5.** Relationship of light-induced leaf adaxial surface temperature increase ( $\Delta T$ ) and the efficiency of light conversion to heat with qZ component of non-photochemical quenching ( $\Delta\text{NPQ}$ ) at constant PAR. Experimentally obtained data (points; black = RGB, red = R, green = G, blue = B chamber) of  $\Delta T$  and  $\Delta\text{NPQ}$  relationship was assessed by subtracting values of adaxial leaf surface temperature (FLIR) or NPQ values (at  $396 \mu\text{mol m}^{-2} \text{s}^{-1}$ , 450 nm) estimated for control and DTT-infiltrated leaves. The theoretical curve (dotted purple line) with confidence band (95%, transparent orange area) and solid line (grey) were calculated based on the Bradley and linear regression model, respectively, employed to fit the experimental data of  $\Delta T/\Delta\text{NPQ}$ . Fitting was applied as specified in Material and Methods and reported with equations and adjusted  $R^2$  ( $R_a^2$ ) values to determine the goodness of data fitting.

## 2.2. Influence of grow light spectra on stomatal traits, gas exchange and abaxial leaf surface temperature

Our previous analysis [12] proved that the replacement of a red light with a green one in the spectrum induces stomatal dimensions contraction. It was especially noted that increasing G light intensity reduced pore area by nearly one-third, reduced stomatal density ( $S_d$ ) when occupied 20-40% of the spectrum and significantly reduced the overall pore area estimated per leaf area. Similarly, this result also showed that green light, applied this time, solely for tomato cultivation influences the distribution of the stomata in the abaxial epidermis (Figure 6).

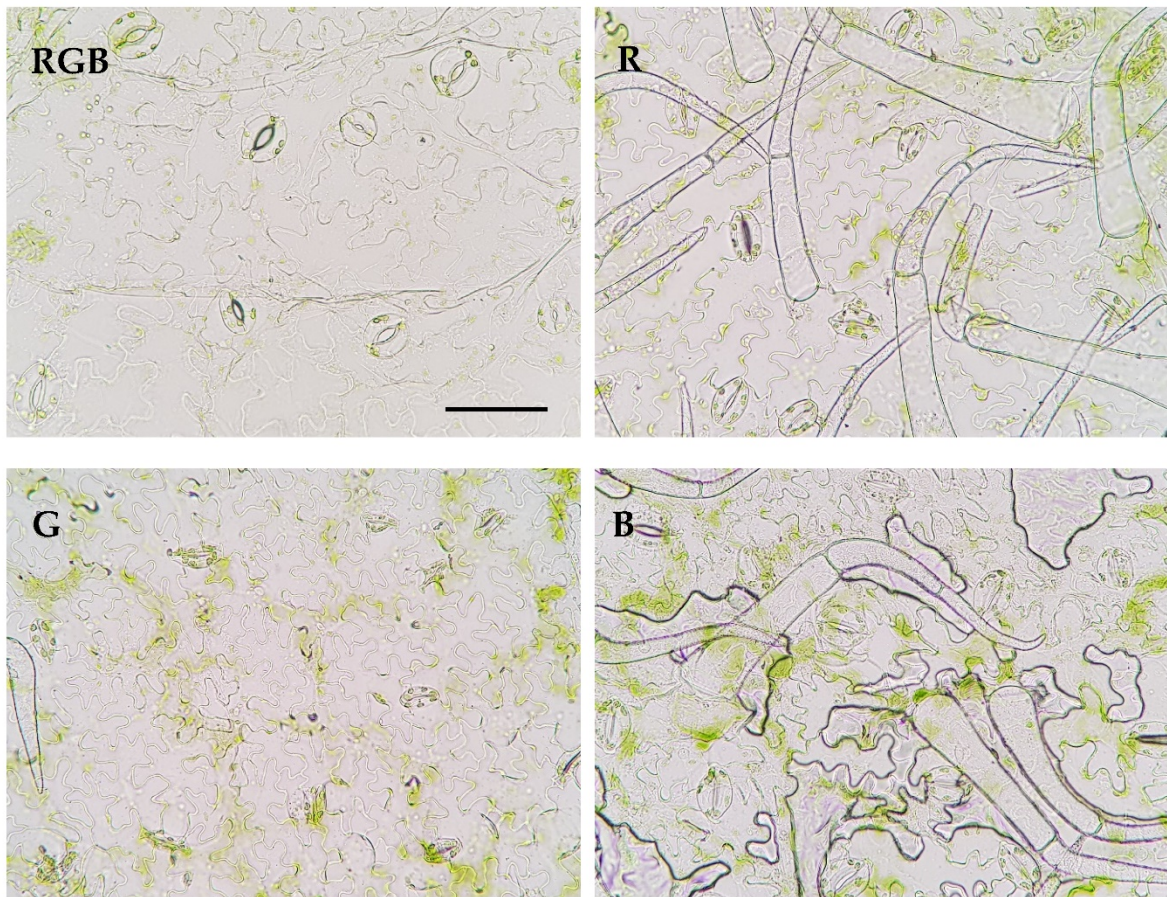


**Figure 6.** Effect of RGB, R, G or B LED light on the distribution of the stomata in the abaxial epidermal layer of 28 DAT tomato plants (*Solanum lycopersicum* L. cv. Malinowy Ozarowski) leaves. Data presented randomly selected images of leaf epidermises obtained by direct peeling taken under the Nikon Eclipse E100 light microscope (see Material and Methods for details), magnification of  $\times 400$ . Bar = 50  $\mu$ m.

As expected, the lowest  $S_d$  was presented in plants, which developed in the presence of G light, while the highest was in R and B light (Table 1). Pore area per leaf area has been also documented to be the highest under R light treatment and the lowest for G light, thus indicating that the effective area of transpiration within G plants was significantly reduced. The reason for this is restricted to both  $S_d$  and the pore width of individual stomata under G treatment (Figure 7, Table 1), compared to other light treatments. As a result, stomatal pores were reduced under G treatment by approximately 50% compared to RGB. At the same time, we documented that the area of the stomatal complex was positively correlated with light intensity and not related to the applied light quality. Interestingly, analyzed abaxial epidermal layers showed some curious phenomenon of trichome pattern presenting unequal distribution under different light treatments (Figure 6), which might interfere with the transpiration rate and consequently modulate foliar temperature. Thus, it requires further investigation in the future. It should be however noted, that despite the R plants showing high pore area per leaf area parameter, the overall area of the abaxial leaf surface was reduced under R light, as

a consequence of the development of smaller leaves. Consequently, the total pore area per total abaxial leaf surface was the highest under RGB and B light and reduced by 34 and 76% in R and G plants, respectively (Table 1).

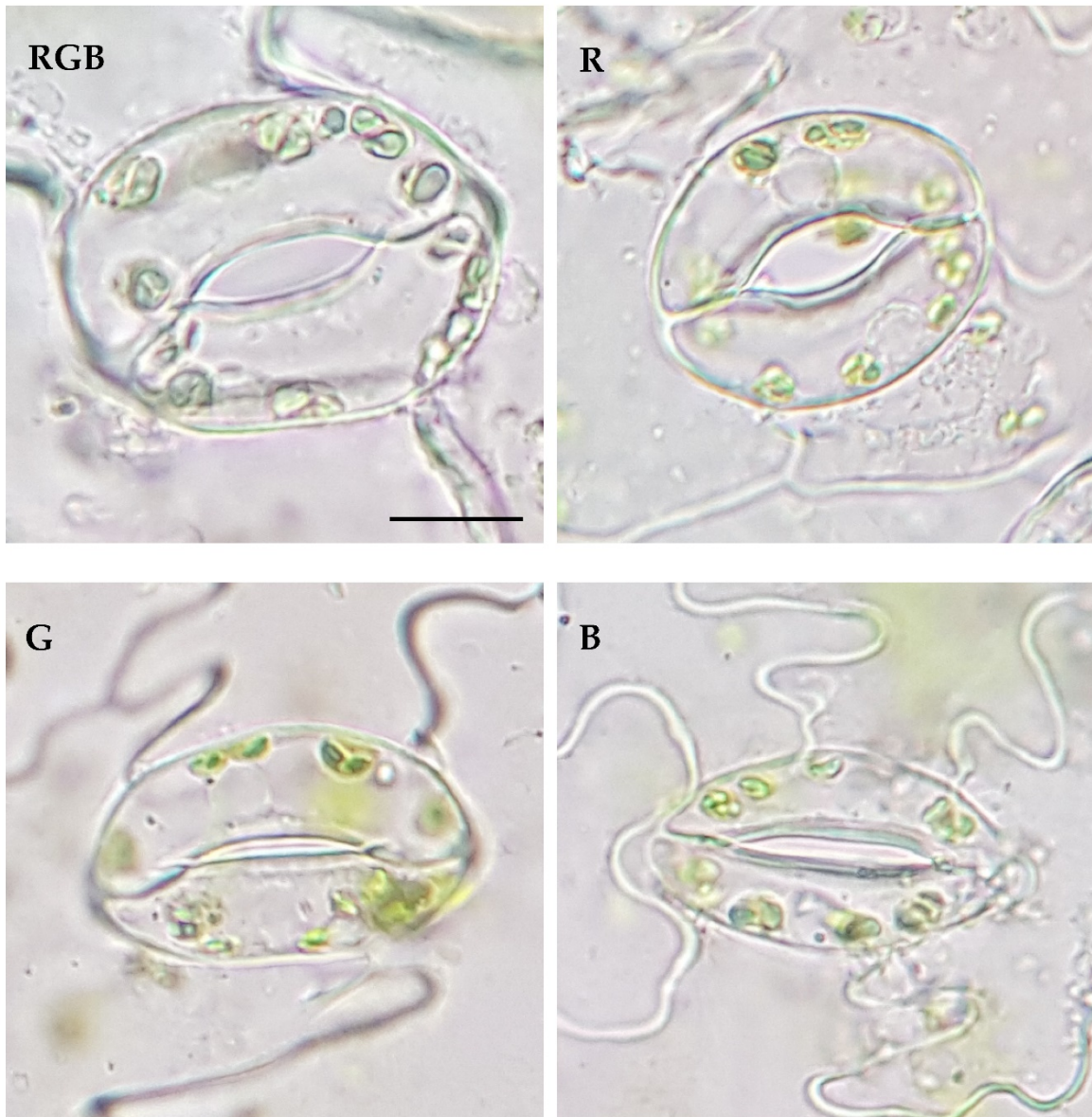


**Figure 7.** Effect of RGB, R, G or B LED light on the anatomy of the stomata in the abaxial epidermal layer of 28 DAT tomato plants (*Solanum lycopersicum* L. cv. Malinowy Ozarowski) leaves. Data presented randomly selected images of leaf epidermises obtained by direct peeling taken under the Nikon Eclipse E100 light microscope (see Material and Methods for details), magnification of  $\times 1000$ . Bar = 10  $\mu\text{m}$ .

**Table 1.** Stomatal traits of 28 DAT tomato plants (*Solanum lycopersicum* L. cv. Malinowy Ozarowski) grown under different light conditions.

Parameter	Treatment			
Stomatal traits (abaxial leaf surface)	RGB	R	G	B
Stomatal complex width ( $\mu\text{m}$ )	24.00 $\pm$ 3.49a	19.39 $\pm$ 1.87b	17.84 $\pm$ 0.81b	17.62 $\pm$ 2.14b
Stomatal complex length ( $\mu\text{m}$ )	29.82 $\pm$ 3.19a	24.24 $\pm$ 2.17b	25.06 $\pm$ 3.42b	26.07 $\pm$ 1.86b
Stomatal width/length ratio	0.80 $\pm$ 0.06a	0.80 $\pm$ 0.04a	0.72 $\pm$ 0.1b	0.68 $\pm$ 0.08b
Stomatal complex area ( $\mu\text{m}^2$ )	568.44 $\pm$ 139.38a	373.63 $\pm$ 59.72b	349.19 $\pm$ 61.03b	347.07 $\pm$ 60.38b
Pore width ( $\mu\text{m}$ )	4.04 $\pm$ 0.88ab	4.34 $\pm$ 0.91a	1.90 $\pm$ 0.67c	3.65 $\pm$ 0.99b

Pore length ( $\mu\text{m}$ )	12.32 $\pm$ 1.59b	12.02 $\pm$ 1.22b	12.26 $\pm$ 2.18b	13.78 $\pm$ 1.62a
Aspect ratio of pores (width/length)	0.33 $\pm$ 0.06a	0.36 $\pm$ 0.07a	0.16 $\pm$ 0.05c	0.26 $\pm$ 0.06b
Stomatal pore area ( $\mu\text{m}^2$ )	34.14 $\pm$ 9.12a	35.27 $\pm$ 8.69a	17.15 $\pm$ 6.00b	29.90 $\pm$ 8.89a
Stomatal density $S_d$ (no. $\text{mm}^{-2}$ )	117.22 $\pm$ 5.08b	140.66 $\pm$ 8.79a	90.84 $\pm$ 13.43c	137.73 $\pm$ 18.30a
Pore area per leaf area ( $\mu\text{m}^2 \text{ mm}^{-2}$ )	4002.09 $\pm$ 1069.27b	4960.61 $\pm$ 1222.53a	1557.91 $\pm$ 545.44c	4100.42 $\pm$ 1219.19b
Total pore area per total leaf surface ( $\mu\text{m}^2 \text{ cm}^{-2}$ )	18019.50 $\pm$ 4814.41a	11952.84 $\pm$ 2945.76b	4321.61 $\pm$ 1513.05c	19751.74 $\pm$ 5872.84a

The values are means of ten replicates  $\pm$  SD. For the individual stomatal traits, a magnification of  $\times 1000$  was used or  $\times 400$  for  $S_d$  and pore area per leaf area/total pore area per total leaf surface. Different letters (a–c) in the same row indicate significant differences between the treatments at  $p = 0.05$  with a Tukey's HSD test.

Analyses of stomatal traits allow a better understanding of recorded differences in gas exchange and abaxial side leaf temperature among groups. Analyses were performed with water- and DTT-infiltrated leaves illuminated under constant  $\text{PAR} = 400 \mu\text{mol m}^{-2} \text{ s}^{-1}$ , corresponding to conditions of NPQ and  $T_{\text{adaxial}}$  measurements. Results of net photosynthetic rate ( $P_n$ ) (Figure 8a) showed similar tendencies to  $F_v/F_m$  values (Figure 3). Plants grown under monochromatic R and G light presented reduced  $\text{CO}_2$  fixation (under RBG light illumination) by 24 and 62% compared to RGB plants, respectively. At the same time, plants grown under monochromatic B light sustained RGB-like levels of  $\text{CO}_2$  fixation. We also recorded that DTT treatment increased  $P_n$  in R and decreased its value in RGB plants, due to influence on stomatal conductance (Figure 8b). Analysed  $g_s$  showed that DTT reduced stomatal conductance by 63, 43 and 29% in RGB, G and B plants, respectively. Consequently, the transpiration rate (Figure 8c) was also reduced after the DTT application in these groups. On the contrary, in R plants DTT enhanced stomatal conductance and transpiration by 24 and 33%, respectively. Moreover, as expected temperatures of the non-illuminated abaxial leaf side measured under  $400 \mu\text{mol m}^{-2} \text{ s}^{-1}$  were lower (Figure 8d) than those of the adaxial side (Figure 4a), which might be considered a consequence of the absence of direct light exposition and cooling effect of transpiration.

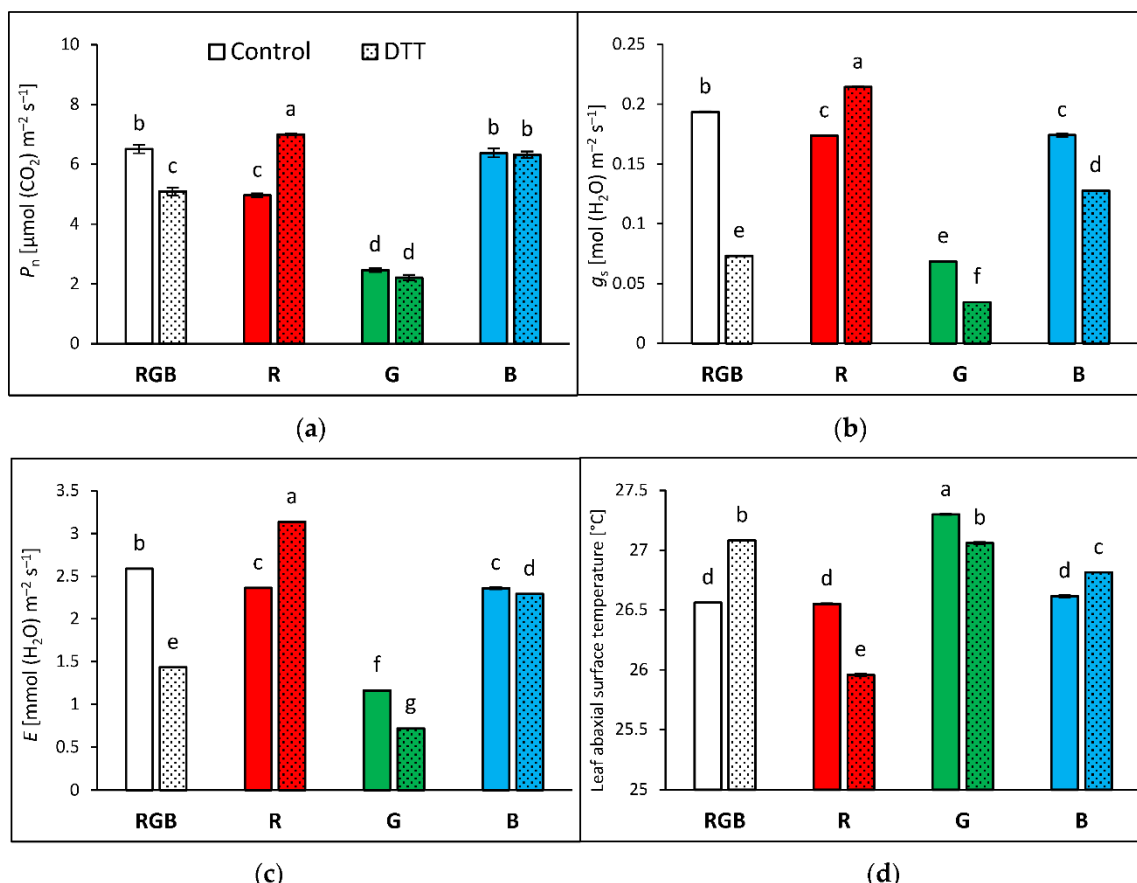


**Figure 8.** Gas exchange parameters measured in the  $2 \times 3$ -cm transparent chamber illuminated with  $400 \mu\text{mol m}^{-2} \text{s}^{-1}$  of the RGB spectrum (R:G:B = 1:1:1) of water- (control) or 5 mM DTT-infiltrated (DTT) leaves of 28 DAT tomato plants (*Solanum lycopersicum* L. cv. Malinowy Ozarowski). Detached leaves were infiltrated for 1 h in the dark, followed by pre-illumination at  $400 \mu\text{mol m}^{-2} \text{s}^{-1}$  of RGB light for the next 30 min. (a) Net photosynthetic rate ( $P_n$ ), (b) stomatal conductance ( $g_s$ ), (c) transpiration rate ( $E$ ) and (d) temperature of leaf abaxial surface. Each bar represents the average  $\pm$  SD of six independent measurements ( $n = 6$ ). Different letters (a–g) indicate significant differences between treatments at  $p = 0.05$  with a Tukey's HSD test.

Nonetheless, a comparison of  $g_s$  and  $T_{\text{abaxial}}$  value in water- and DTT-infiltrated samples of RGB, R and B plants indicated a sort of positive relationship. The curve plotted in Figure 9, obtained by fitting experimental data of  $g_s$  and  $T_{\text{abaxial}}$ , presents satisfactorily high goodness of data fitting with adjusted  $R^2$  of 0.984, thus providing direct evidence of a close connection between  $g_s$  and  $T_{\text{abaxial}}$ .

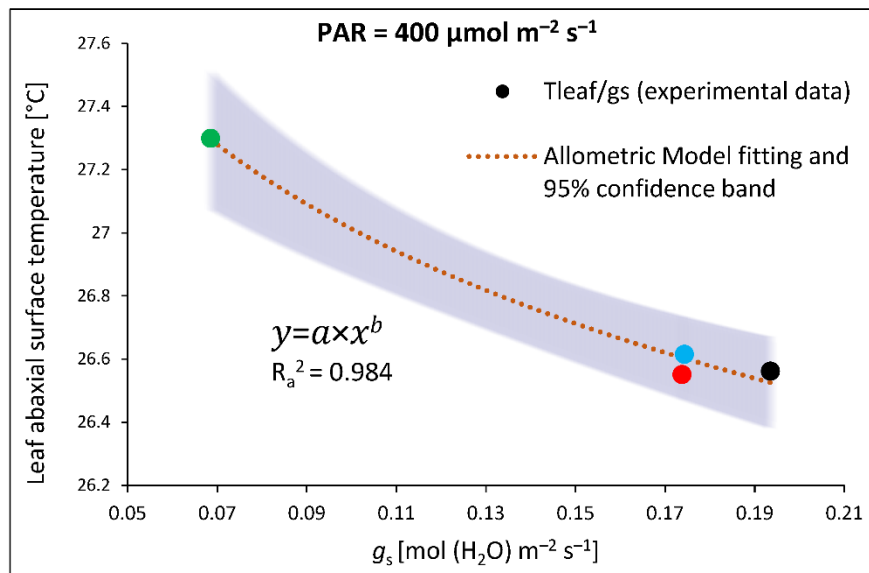


**Figure 9.** Relationship of leaf abaxial surface temperature ( $T_{\text{abaxial}}$ ) and the stomatal conductance ( $g_s$ ) at constant PAR. Experimentally obtained data (points; black = RGB, red = R, green = G, blue = B chamber) of  $T_{\text{abaxial}}$  and  $g_s$  relationship were assessed with  $400 \mu\text{mol m}^{-2} \text{s}^{-1}$  of the RGB spectrum (R:G:B = 1:1:1). The theoretical curve (dotted orange line) and confidence band (95%, transparent purple area) were calculated based on the Allometric model employed to fit the experimental data of  $T_{\text{abaxial}}/g_s$ . Fitting was applied as specified in Material and Methods and reported with equation and adjusted  $R^2$  ( $R_a^2$ ) value to determine the goodness of data fitting.

### 2.3. Influence of grow light spectra on gas exchange and abaxial leaf surface temperature in response to increasing light intensity (LC)

Analysed relationship of  $T_{\text{abaxial}}$  and  $g_s$  at constant light intensity showed their close relation (Figure 9). Thus, in the next experiment, we have assessed the relationship between foliar temperature and stomatal conductance in response to increasing light intensity, to determine the light intensity above which cooling effects of transpiration become limited. To overcome stomatal conductance limitation, we applied the procedure of a rapid light response curve with pre-illuminated leaves and a stepwise decrease of light intensity (LC). The drawback of such an assay is an overestimation of stomata openness compared to the measurement at constant PAR without previous pre-illumination. However, the primary reason to conduct such an experiment was to estimate the threshold level of PAR above which the close relationship of  $g_s$  and foliar temperature regulation tends to fail. Results of gas exchange measurements showed that the rate of net photosynthesis (Figure 10a), stomatal conductance (Figure 10b) and transpiration (Figure 10c) is the highest in B plants and the lowest in plants grown under G light. To plot curves, we employed

regression models fitting experimental data and showed that  $P_n$  reached a plateau at  $\text{PAR} \geq 800 \mu\text{mol m}^{-2} \text{s}^{-1}$ , while  $g_s$  at  $\text{PAR} \geq 400 \mu\text{mol m}^{-2} \text{s}^{-1}$ , in all light treatments. At the same time, transpiration rate (Figure 10c) and abaxial leaf temperature (Figure 10d) rise continuously in response to PAR increase. Thus, we observed a steady increase in abaxial side temperature despite the concomitant increase in transpiration, indicating that the cooling effect of transpiration at higher PAR become limited.

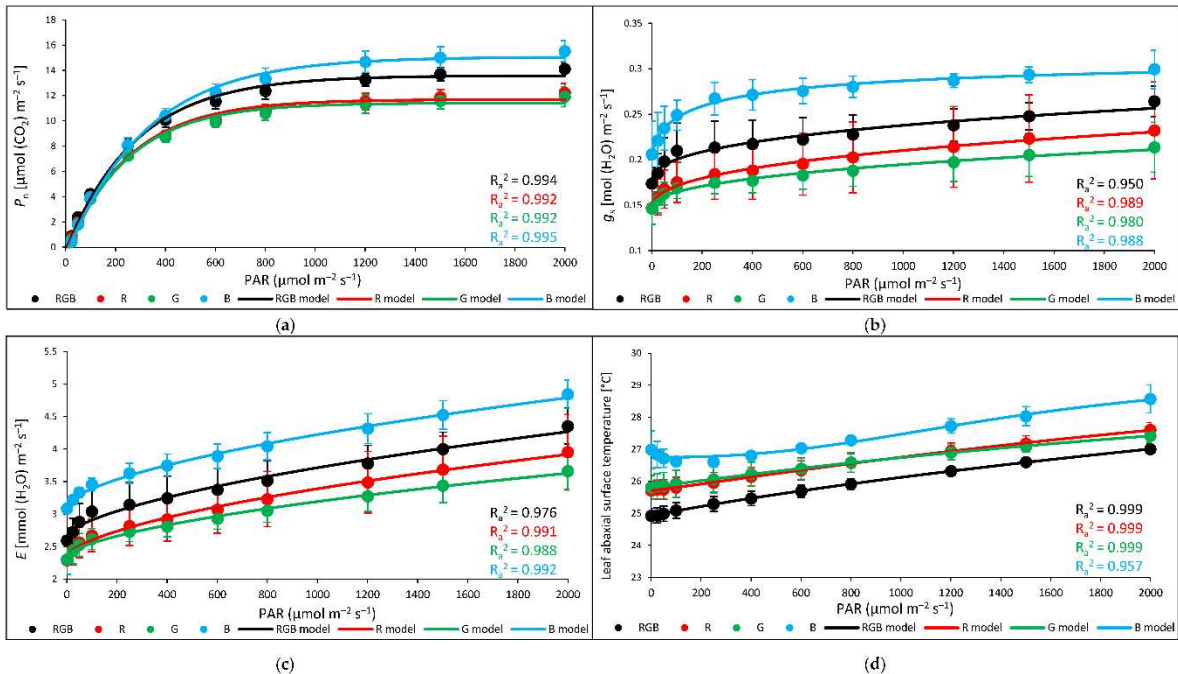


**Figure 10.** Gas exchange parameters measured with LED light source 6400-02B illuminated with 0–2000  $\mu\text{mol m}^{-2} \text{s}^{-1}$  of the RB light (R:B 10:1) of control leaves of 28 DAT tomato plants (*Solanum lycopersicum* L. cv. Malinowy Ozarowski). (a) Net photosynthetic rate ( $P_n$ ), (b) stomatal conductance ( $g_s$ ), (c) transpiration rate ( $E$ ) and (d) leaf abaxial surface temperature. Each data point represents the average  $\pm$  SD of six independent measurements ( $n = 6$ ). We employed (a) an asymptotic regression model, (b,c) a lognormal cumulative distribution function and (d) a logistic regression model to fit the experimental data (points; black = RGB, red = R, green = G, blue = B chamber) of gas exchange parameters against PAR. Fitting was applied as specified in Material and Methods and reported with adjusted  $R^2$  ( $R_a^2$ ) values to determine the goodness of data fitting.

Also, the analysed water-use efficiency (WUE), which expresses the trade-off between carbon assimilated as biomass or grain and unit of water release [22] showed that the efficacy of water utilization increased up to approximately 800  $\mu\text{mol m}^{-2} \text{s}^{-1}$  of PAR. Results showed that for all light treatments, both intrinsic water-use efficiency ( $P_n/g_s$ ) ( $\text{WUE}_{\text{int}}$ ) (Figure 11a) and instantaneous water-use efficiency ( $P_n/E$ ) ( $\text{WUE}_{\text{ins}}$ ) (Figure 11b) increased rapidly within lower light intensity until reaching the maximum value of WUE. In the case of  $\text{WUE}_{\text{ins}}$  the lowest water-use efficiency was noted for B plants, but without statistically significant differences recorded among groups, while when analysed  $\text{WUE}_{\text{int}}$  B plants presented decreased water-use efficiency in response to 200–1000  $\mu\text{mol m}^{-2} \text{s}^{-1}$  compared to other plants.

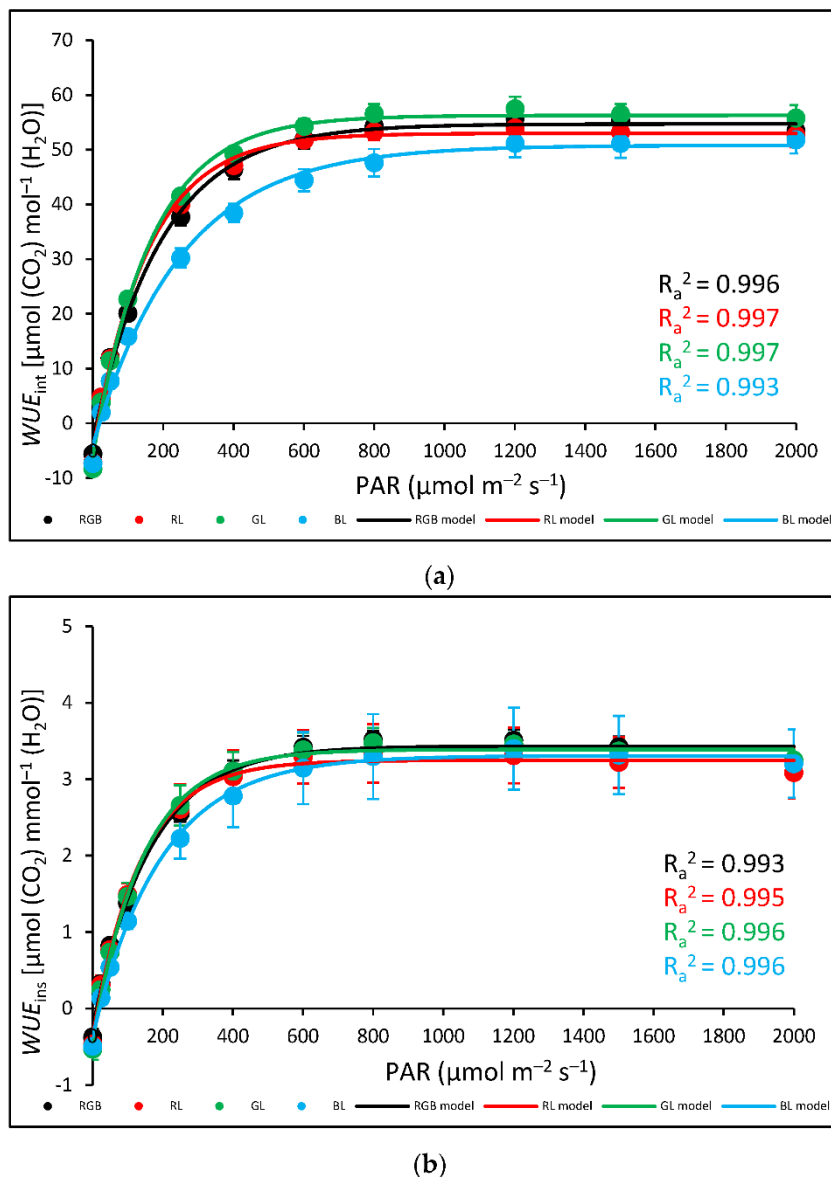


**Figure 11.** Gas exchange parameters measured with LED light source 6400-02B illuminated with 0–2000  $\mu\text{mol m}^{-2} \text{s}^{-1}$  of the RB light (R:B 10:1) of control leaves of 28 DAT tomato plants (*Solanum lycopersicum* L. cv. Malinowy Ozarowski). (a) intrinsic water-use efficiency ( $P_n/g_s$ ) ( $WUE_{int}$ ), (b) instantaneous water-use efficiency ( $P_n/E$ ) ( $WUE_{ins}$ ). Each data point represents the average  $\pm$  SD of six independent measurements ( $n = 6$ ). We employed (a) an asymptotic regression model and (b) a sigmoidal model to fit the experimental data (points; black = RGB, red = R, green = G, blue = B chamber) of gas exchange parameters against PAR. Fitting was applied as specified in Material and Methods and reported with adjusted  $R^2$  ( $R_a^2$ ) values to determine the goodness of data fitting.

The threshold level of  $g_s$  influence on the leaf abaxial surface temperature of plants is documented in Figure 12. Curves plotted with experimental data fitting for each chamber presented that, while the mechanism of stomatal openness effectively stabilizes abaxial temperature at lower PAR, it starts to fail above approximately 400  $\mu\text{mol m}^{-2} \text{s}^{-1}$  (encircled data points), despite the fact of continuously rising rate of transpiration.

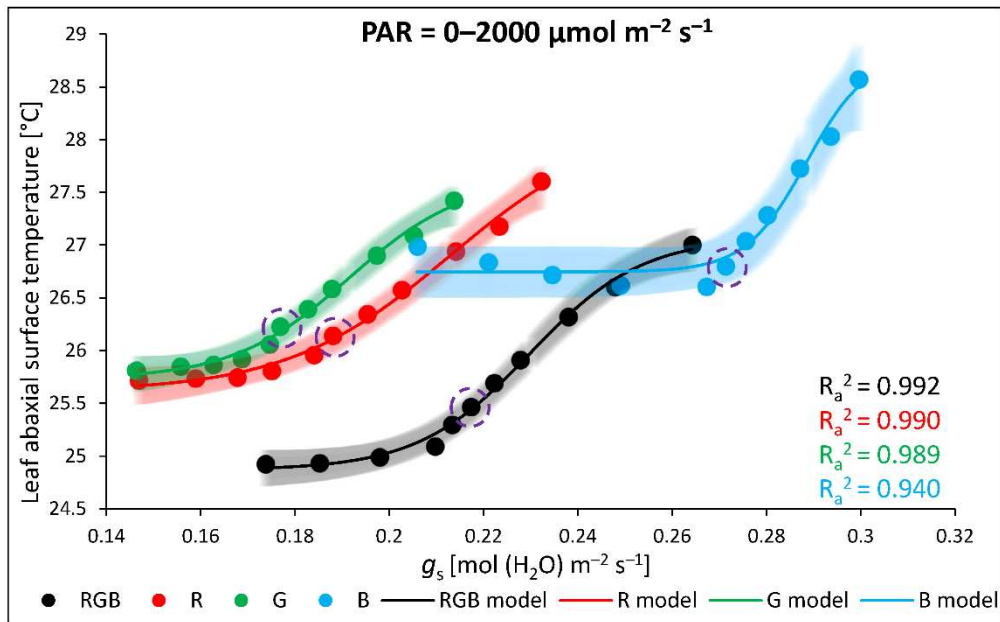


**Figure 12.** Relationship of leaf abaxial surface temperature ( $T_{\text{abaxial}}$ ) and the stomatal conductance ( $g_s$ ) at increasing PAR. Experimentally obtained data (points; black = RGB, red = R, green = G, blue = B chamber) of  $T_{\text{abaxial}}$  and  $g_s$  relationship were assessed with 0–2000  $\mu\text{mol m}^{-2} \text{s}^{-1}$  of the RB light (R:B 10:1). Threshold level of  $g_s$ -related cooling effect limitation is depicted with data points enclosed with purple circle at 400  $\mu\text{mol m}^{-2} \text{s}^{-1}$  of PAR. The theoretical curves (solid line) and confidence bands (95%, transparent area) were calculated based on the log-logistic equation with a variable Hill slope model employed to fit the experimental data of  $T_{\text{abaxial}}/g_s$ . Fitting was applied as specified in Material and Methods and reported with adjusted  $R^2$  ( $R_a^2$ ) value to determine the goodness of data fitting.

### 3. Discussion

It has been previously reported [23] that long-term light-quality treatment has an impact on photosynthetic properties in rice. Authors showed that even under moderate incident light levels (300  $\mu\text{mol m}^{-2} \text{s}^{-1}$ ) monochromatic red and even more blue light enhanced NPQ induction compared to white light treatment. Another study [24] also concluded that NPQ, which is considered important for short-term light acclimation, is also an important mechanism for long-term light acclimation. Similarly, in our previous research [3] we documented that both R and B light long-term treatment increases NPQ amplitude, while G and RGB light lowers its value, due to reduced accumulation of NPQ-related proteins. At the same time, previous research [12,25–28] documented that the quality of growth light influences gas exchange, especially due to modification of stomatal development and movement. The main conclusions results from these studies are that B light stimulates stomata opening more than R one, while the addition of G light to the spectrum reduces stomatal conductance by both contractions of stomata dimension and density, as well as the reduced stomatal openness. Thus, firstly the influence of growth light composition on NPQ and  $g_s$  is well established, and secondly, the effect of these mechanisms on foliar temperature was also noticed [7,8,11,29,30]. Nonetheless, relatively little research exists that analyses the direct influence of the NPQ and  $g_s$  on the leaf surface temperature, because of the different spectral characteristics applied during plant cultivation. In particular, the crucial question to be answered is to identify the mechanism that overrides foliar temperature regulation, try to evaluate its limits, and link it to the long-term exposition of plants to the growth spectrum.

### 3.1. Effect of long-term exposition of tomato plants to different light compositions on maximum PSII photochemical efficiency

In the present study, we have demonstrated that growth-light composition influenced the subsequent maximum PSII photochemical efficiency Fv/Fm, the amplitude of non-photochemical quenching and consequently the adaxial surface temperature of leaf lamina. In agreement with previous reports [3,31] we documented that B light applied both as an exclusive light source or in combination with R and G light increased Fv/Fm. At the same time, results showed that monochromatic R light exerted the most adverse effects on Fv/Fm. Another study [32] documented that the photosynthetic apparatus of potato plantlets under monochromatic R light was impaired compared to those grown under monochromatic B or combined RB spectrum. Also, authors [33,34] documented adverse effects of monochromatic R light on Fv/Fm. Such a phenomenon is called “red-light syndrome” and explained that it is evoked when plants are grown solely under R light [35]. Symptoms of the syndrome include a strong decrease in photosynthetic capacity and Fv/Fm as well as the unresponsive stomata. The observed response is related to the reduced number of chloroplast and thinner layers of mesophyll tissues, resulting in lower photosynthetic capacity. Interestingly, in our research R-grown plants also exerted some morphological features related to red-light syndrome such as leaf curling (data not shown). Furthermore, we have documented that only in R plants application of DTT increase Fv/Fm, while in other plants lowered its value. Similar tendencies have been documented in our previous research [3]. Authors [36] stated that DTT treatment might shift the balance of excitation energy distribution between PSI and PSII, increasing energy partitioning to PSII. Additionally, research [37] showed that DTT as a reductant agent interferes with chloroplast redox state, thus reducing the photoprotective energy-spillover from PSII to PSI, which results in higher Fv/Fm value. The mentioned relationship between long-term acclimation to spectrum composition and energy balance between PSII and PSI is related to the major light-harvesting complex (LHCII) association with each photosystem [38]. Association of most of the LHCIIIs with PSII causes increased absorption of light in the blue region of the spectrum by PSII compared to R light, while partial migration of LHCIIIs to PSI allows for more equal absorption in blue and red spectrum with both photosystems [39]. Overall, we concluded that the application of B light of 435 nm as a sole light source or RGB component exerted a positive influence on photochemical capacity due to more efficient energy partitioning between PSII and PSI, while the opposed trend was observed for monochromatic R light of 662 nm. In the case of monochromatic G light of 520 nm, the observed reduction of Fv/Fm value is related to reduced chlorophyll content and has been documented previously [3,40].

### 3.2. Effect of long-term exposition of tomato plants to different light compositions on energy quenching and adaxial leaf surface temperature

Contrary to our expectation, we found no differences among the foliar temperature of the upper leaf side when measured directly inside chambers (*in situ*), despite the difference in photon flux and spectral characteristics among RGB and G or B light. At the same time, we noted on average 1.0 °C higher within the plants grown under monochromatic R light. Overall, foliar temperature measured *in situ* in all light treatments was noted within 1.5–2.5 °C below the air temperature. According to previous analysis [41], if plants are not water stressed, the radiation source exerts a much smaller effect than plant water status and leaf evaporative cooling. However, when the cooling mechanism decreases or becomes inefficient the leaf temperature can increase well above the ambient temperature [41].

Thus, we evaluated the foliar temperature change in response to increasing photon flux in the next experiment. Our previous research showed that long-term exposure to G light compared to B or R light significantly reduces the accumulation of NPQ-related protein and consequently its amplitude and heat dissipation [3]. The previous study [42] stated that terrestrial plants are rather fine-tuned to reduce energy absorption and developed excessive pigments such as carotenoids and anthocyanins that effectively reduce the flux of mostly shortwave (including B light) PAR, containing much of the surplus energy. At the same time, the R and B light photons are absorbed more strongly by

photosynthetic pigments than G photons, thus their absorption near the adaxial surface also increases heat dissipation [43]. In such a scenario, it is expected that in a high light intensity background, additional R or B light causes up-regulation of NPQ-related heat dissipation and increased  $T_{leaf}$  [43].

Based on these assumptions, we have decided to test whether the spectrum composition influenced NPQ amplitude when analysed in response to increasing PAR and consequently affected the upper leaf side temperature. To this end, however, we applied blue actinic light during NPQ measurements of plants grown under different spectra and observed differences among groups as well as the positive correlation with the extent of NPQ and FLIR-recorded adaxial leaf surface temperature (Figure 4a). The highest  $T_{adaxial}$  in control was noted for the B light tomato plants presenting consequently the highest NPQ amplitude, while the lowest values were noted for the G group. Furthermore, this positive correlation of spectrum-related  $T_{adaxial}$  and NPQ values was also proved with the subsequent analyses of DTT-infiltrated leaves documenting that reduced NPQ interfered with lowered leaf temperature (Figure 4b). Previously, authors [8] also reported the correlation between the extent of NPQ and light-induced temperature increase in tobacco leaves. On the contrary, research [11], documented no direct correlation between the PsbS-related NPQ amplitude and the foliar temperature dynamics. Such a conclusion might be, however, a sort of oversimplification, because authors [44] identified two independent quenching sites depending on PsbS or zeaxanthin, while another studies [17,45–47] documented that both PsbS-deficient (*npq4*) as well as zeaxanthin-deficient (*npq1*) *Arabidopsis* plants showed a similar reduction of the maximum NPQ level compared to wild type plants. Another feasible way of dissipation of absorbed energy such as carotenoid radical cation formation (qZ) was also postulated [11]. According to authors [17], both PsbS and Z are crucial elements of photoprotective energy dissipation, but their role is different. PsbS protein interferes with the formation of densely packed aggregates of thylakoid membrane proteins, thus allowing the exchange and incorporation of xanthophylls. At the same time, zeaxanthin formation in place of V with VDE enhanced direct excitation quenching.

Based on these results, applied DTT allowed to inhibit VDE activity and proved the influence of a more slowly inducible zeaxanthin-dependent component of non-photochemical quenching on the subsequent foliar temperature with both linear and non-linear fitting model presenting satisfactorily high goodness of data fitting (Figure 5). Moreover, analyses of NPQ and  $T_{adaxial}$  in DTT-infiltrated leaf as well as our previous analyses of PsbS and VDE levels under different spectra [3] proved that the relationship between PsbS-dependent NPQ amplitude and  $T_{leaf}$  regulation is minor when Z accumulation is inhibited (Figure 4b).

### 3.3. Effect of long-term exposition of tomato plants to different light compositions on gas exchange parameters, stomatal traits and abaxial leaf surface temperature

At the same time, the role of stomatal conductance in leaf energy balance cannot be omitted. However, as previous analyses [48] documented that stomata in leaves of tomato plants are predominantly placed on the abaxial side, we recorded the relationship between  $g_s$  and  $T_{abaxial}$  with IRGA and thermocouple, respectively. Such an approach has advantages, as it allows us to measure the straightforward influence of light-regulated stomatal openness on abaxial leaf side temperature and minimize the effect of direct illumination on temperature change. In previous studies [11], authors concluded that foliar temperature dynamics are primarily affected by stomatal aperture in response to intense irradiation. The authors, however, estimated stomatal aperture indirectly with crop water stress index (CWSI) indicator, while the FLIR-recorded  $T_{leaf}$  was monitored for the adaxial side, which is less occupied by stomata. Unfortunately, the CWSI indicator could overestimate the  $g_s$ , thus a new thermal indicator of stomatal conductance (GSI), as a more reliable tool for indirect stomatal conductance estimation has been proposed [1]. In our research, however, we documented negative non-linear correlations within directly and simultaneously recorded  $T_{abaxial}$  and  $g_s$  under constant PAR (400  $\mu\text{mol m}^{-2} \text{s}^{-1}$ ) (Figure 9) presenting satisfactorily high goodness of data fitting with adjusted  $R^2$ . However, when data was analysed with increasing light intensity this correlation became less obvious (Figure 10b–d). It was found that above the 400  $\mu\text{mol m}^{-2} \text{s}^{-1}$  of PAR stomata seemed to approach their maximal aperture and the cooling effect, which has been stabilizing the abaxial side

temperature in lower PAR (Figure 8), tended to fail (Figure 12), although the transpiration rate was still increasing (Figure 10c). Moreover, the recorded negative non-linear correlation between  $g_s$  and  $T_{abaxial}$  under constant PAR (Figure 9) is also disturbed when analysed within the light response curve (LC). We found, that within LC the highest  $T_{abaxial}$  was noted for B-grown plants (Figure 10d) presenting, at the same time, the highest  $g_s$  and transpiration rate (Figures 10b, c), while the lowest  $T_{abaxial}$  was presented in RGB plants. Additionally, analysed WUE parameters (Figure 11) confirmed that enhanced  $P_n$  during LC noted for B plants, which had resulted from the higher stomatal conductance, reduced, however, the efficiency of water use per unit of carbon dioxide fixed. Interestingly, comparing the influence of spectrum on  $g_s$  noted under constant PAR (Figure 8b) and LC (Figure 10b), we showed that stomata of B-grown plants presenting enhanced responsiveness to increasing light intensity compared to RGB, which cannot be simply explained by differences of stomatal traits. Consequently, based on analysed stomatal traits (Table 1), we concluded that the size of the stomata complex is related to applied light intensity, while the stomatal density and pore area are affected by light quality. Both monochromatic R and B light enhanced the  $S_d$ . At the same time, however, stomata of R plants remain significantly less sensitive to higher PAR, and that such a response has been postulated to be a trace of red-light syndrome [35]. Furthermore, we documented, that long-term exposition of tomato to monochromatic G light caused a reduction of stomatal aperture within the pore width, while G and G-enriched spectrum significantly lowered the number of stomata per abaxial leaf area. Consistent with our data, previous studies [33] also documented that, B light facilitates stomatal opening and density compared with G light treatment. Moreover, as the G light reverses the effect exerted by B light, its addition to the RB spectrum could enhance the drought tolerance by altering stomatal aperture [49] and reduction of stomatal density, which has been documented within RGB treatment in this study. The disadvantage of monochromatic G light application for plant cultivation is reduced  $P_n$  and increased  $T_{abaxial}$ , resulting from significantly lower stomatal conductance. It has been shown [33] that monochromatic light of each kind modifies the hormonal balance within the leaf. Authors concluded that the mechanism of B light regulates  $g_s$  is related to a decreased abscisic acid (ABA) level under B light, whereas G light enhanced ABA level and ABA-sensitivity due to up-regulation of ABA-responsive element-binding proteins (AREB1) [49].

#### 4. Materials and Methods

##### 4.1. Plant Material and Growth Conditions

Tomato (*S. lycopersicum* L. cv. Malinowy Ozarowski) seeds were germinated in Petri dishes on sterile filter papers soaked in Milli-Q-water at 26 °C. For analysis, a tomato cultivar with reduced leaf dissection (potato leaf phenotype) [50] was chosen to maximize light absorption in the upper part of the canopy. The two-week-old seedlings were transplanted to P9 containers (9 × 9 × 10 cm) and filled with the substrate (white and black peat, perlite, and N:P:K = 9:5:10; pH 6.0–6.5), divided into groups, and transferred to environmentally controlled growth chambers, with non-reflective black separators to eliminate light contamination. The plants were grown for the next 28 consecutive days (28 DAT, days after transplanting) under LED RhenacM12 lamps (PXM, Podleze, Poland) delivering 180  $\mu\text{mol m}^{-2} \text{s}^{-1}$  of the RGB spectrum (R:G:B = 1:1:1) or 80  $\mu\text{mol m}^{-2} \text{s}^{-1}$  of each monochromatic R, G or B light (Figure 1). LED characteristics were as follows: red LEDs: peak wavelength 662 nm, peak broadness at half peak height 22 nm (649–671 nm); green LEDs: 520, 34, 505–539 nm; and blue LEDs: 435, 17, 426–443 nm. RGB treatment was used as the control group. Light composition and photosynthetic photon flux density (PPFD) were monitored daily by a calibrated spectroradiometer GL SPECTIS 5.0 Touch (GL Optic Lichtmesstechnik GmbH, Weilheim/Teck, Germany). The readings were averaged for six locations at the level of the apical bud and maintained by adjusting the distance between the light sources and the plant's canopy. The containers with tomato plants cultivated under the same light treatment were turned twice a day. To avoid canopy shading and overlapping five plants per square meter of the illuminated area were cultivated. The photoperiod was 16/8 h (day/night; day 6:00 a.m.–10:00 p.m.), the average air temperature was maintained at 22/20 °C (day/night), relative air humidity was kept at 50–60% and  $410 \pm 10 \mu\text{mol mol}^{-1}$  of  $\text{CO}_2$ . The plants were watered with tap

water when necessary and fertilized once a week with 1% (w/v) tomato fertilizer (N:P:K = 9:9:27; Substral Scotts, Warszawa, Poland). The fourth leaf from the above plants 28 DAT was used for subsequent analyses. All analyses were conducted between 8:00 a.m. and 12:00 p.m. Ten tomato plants (two repetitions with five plants per light condition) were grown with each kind of light treatment.

#### 4.2. Pre-Illumination of Dithiothreitol-Infiltrated Leaf Samples

DTT (Sigma-Aldrich, St. Louis, MO, USA) pre-treatment of leaves was used to inhibit the VDE that promotes the qZ component of NPQ induction related to V de-epoxidation to Z [3]. At the same time, DTT does not interfere with the development of the trans-thylakoidal  $\Delta$ pH regulating qE related to PsbS protein [37], which has been previously analysed [11].

Fully developed detached leaves of 4 weeks DAT tomato plants were placed immediately in a 2 ml plastic tube with a hole in the lid for leaf petiole, which contained 5 mM DTT solution or distilled water (C, control) [51] for 1 h in the dark. To avoid light contamination leaves were cut off directly under the lighting conditions of the chambers.

After infiltration, C and DTT leaves of each chamber were pre-illuminated for 30 min with RGB light (R(627 nm): G(530 nm): B(447 nm) = 1:1:1) at a light intensity of approximately  $400 \pm 5 \mu\text{mol m}^{-2} \text{s}^{-1}$  (LED Light Source SL-3500 lamp, Photon Systems Instruments, Drasov, Czech Republic). Light intensity and exposure periods applied for pre-illumination were chosen based on previous analyses [3,17,45,52] to allow for the acceleration of NPQ formation and to avoid PSII photoinhibition. Subsequently, leaves were re-darkened for 15 min to allow relaxation of the trans-thylakoid pH gradient without substantial reconversion of Z back to V.

#### 4.3. Rapid Light Curve (RLC) of Chlorophyll Fluorescence (ChF) Analyses

ChlF was measured using a pulse amplitude-modulated (PAM) fluorometer (Maxi IMAGING PAM M-Series, Walz, Effeltrich, Germany) on the adaxial side of the leaf samples placed in plastic tubes. To avoid heterogeneity of DTT infiltration, six circle-shaped areas of interest (AOIs) were selected and averaged for each replicate. The minimal (dark) fluorescence level (Fo) was measured using measuring modulated blue light (450 nm,  $0.01 \mu\text{mol m}^{-2} \text{s}^{-1}$ ). The maximal fluorescence level (Fm) with all PSII reaction centres closed was determined by a 0.8 s saturating blue light pulse (SP = 450 nm) at  $5000 \mu\text{mol m}^{-2} \text{s}^{-1}$  in 30 min dark-adapted samples. The maximum PSII photochemical efficiency (Fv/Fm) was derived from that ( $\text{Fv/Fm} = (\text{Fm} - \text{Fo})/\text{Fm}$ ). Then, for quenching analysis, leaf samples were illuminated for approximately 5 min at increasing blue actinic light intensity (AL = 450 nm) at the following steps: 0, 20, 55, 110, 185, 280, 335, 395, 460, 530, 610, 700, 925 and  $1250 \mu\text{mol m}^{-2} \text{s}^{-1}$  [53]. Increasing AL intensity during the measurement of C- and DTT-fed leaves was chosen to clarify the role of qZ and qE in the  $T_{\text{leaf}}$  regulation of plants grown under different light regimes while illuminating with excess energy excitation. To determine the NPQ induction, SPs ( $5000 \mu\text{mol m}^{-2} \text{s}^{-1}$ , duration 0.8 s) were applied every 20 s during each given AL intensity. To avoid qI induction RLC assay was shortened to 5 min. Fluorescence yields obtained during the analysis were combined to calculate the Stern–Volmer  $\text{NPQ} = (\text{Fm} - \text{Fm}')/\text{Fm}'$  (where Fm' is the maximal level of chlorophyll fluorescence in light) [54]. The assessed NPQ value exceeded unity; thus, its value is presented as  $\text{NPQ}/4$ . All measurements of ChlF were carried out at a constant ambient temperature of  $25 \pm 1^{\circ}\text{C}$ . Each measurement comprised six replicates.

#### 4.4. Determination of Leaf Temperature with FLIR

The temperature of the leaf surface was determined as previously described [7,8,11] with a FLIR E50 camera software (Systems, Wilsonville, USA) that detects temperature with a relative resolution of  $0.05^{\circ}\text{C}$  based on measurement of infrared radiation at  $7.5\text{--}13 \mu\text{m}$ . The camera operates on the principle of object scanning that gives a spatial resolution of  $320 \times 240$  pixels images recorded to a disk in the thermal camera. The pictures were captured with the maximal frequency of image refreshing (60 Hz). For analyses leaves of similar size, age, and shape from each light regime were

chosen. Infrared imaging of  $T_{leaf}$  ( $T_{adaxial}$ ) was recorded on the adaxial leaf surface either under the chamber-specific light and air temperature (at  $22 \pm 1$  °C) conditions or performed simultaneously during chlorophyll fluorescence imaging (at  $25 \pm 1$  °C) after the NPQ parameter reached a plateau phase of induction at  $396 \mu\text{mol m}^{-2} \text{ s}^{-1}$ , according to previous results [7]. Each measurement comprised six replicates.

#### 4.5. Stomatal Traits in the Various Lighting Spectra

Previous research [12] concluded that in response to increasing G light intensity in the spectrum, the plants tended to contract their stomatal dimension and consequently reduced  $g_s$ . Thus, in the present study, we analysed plants grown solely under monochromatic lights (R, G, and B) or mixed RGB to elusive which applied light exerts the most pronounced effects on the stomata.

The leaf epidermal strips from 28 DAT plants were used for all morphological stomatal features. Ten randomly selected leaves (one leaf per plant) per light treatment were collected in the morning and the epidermal strips (four strips per leaf) were peeled off from the abaxial side of the leaf (avoiding leaf veins) and were allowed to float on 2 ml of a basal reaction mixture (5 mM (2-(N-morpholino)ethanesulfonic acid, MES), 50 mM KCl, 0.1 mM CaCl<sub>2</sub>, pH 6.5) for 2 h [55]. Stomatal traits were analysed with the images obtained by a Nikon Eclipse E100 microscope with AxioVision 4.8 software (Carl Zeiss Inc., Oberkochen, Germany). A magnification of  $\times 1000$  was used for the individual stomatal traits, and ten randomly selected stomata per sampling area were measured. The stomatal complex width, length, pore width (minor axis of the pore), pore length (major axis of the pore) and stomatal width/length ratio were measured. For the width/length ratio, stomata width, including pore width, was chosen instead of the guard cell width, since the latter changes as the stomata close. The stomatal and stomatal pore area ( $\mu\text{m}^2$ ) were also determined using AxioVision 4.8. Stomatal density ( $S_d$ ) was determined under a magnification of  $\times 400$  with five different fields of view per sampling area. Pore area per leaf area was calculated as the pore area per stomata  $\times S_d$ , and total leaf pore area as a cumulative pore area of the stomata (based on  $S_d$ ) to the total abaxial leaf surface [26,56].

#### 4.6. Leaf Gas Exchange and Temperature Determination of Plants Grown in the Various Lighting Spectra

The photosynthetic parameters were measured using a Li-6400XT Portable Photosynthesis System (LI-COR Inc., Lincoln, USA) with the 2  $\times$  3-cm transparent chamber (6400-08) illuminated directly with the RGB chamber-like light composition or with 2  $\times$  3-cm LED light source 6400-02B ( $665 \pm 10$  nm and  $470 \pm 10$  nm) for light response curve (LC). The leaf cuvette conditions were maintained at a relative air humidity of 60%,  $400 \mu\text{mol mol}^{-1}$  of external CO<sub>2</sub> concentration, gas flow rate of  $500 \pm 2 \mu\text{mol s}^{-1}$  and block temperature set to constant 25 °C. Analyses with the transparent gas chamber were conducted under  $400 \mu\text{mol m}^{-2} \text{ s}^{-1}$  of the RGB spectrum (R:G:B = 1:1:1) with 300 s per replicate to stabilize gas exchange. For the LC analysis, we applied the procedure of rapid light response curve with pre-illuminated leaves (see 4.2. *Pre-Illumination of Dithiothreitol-Infiltrated Leaf Samples*) and stepwise decrease of light intensity at the following steps: 2000, 1500, 1200, 800, 600, 400, 250, 100, 50, 25 and 0  $\text{m}^{-2} \text{ s}^{-1}$ . During the LC steps were time-separated (200 s) to stabilize gas exchange. The applied procedure of rapid light curve, despite its short time of sampling and high responsiveness to drops in the light intensity, has some drawbacks. The method tends to overestimate stomata openness due to its slower adjustment to the actual light level. Despite that, we successfully applied it to evaluate the relationship between  $g_s$  and  $T_{leaf}$ .

The values of the net photosynthetic rate ( $P_n$ ), stomatal conductance ( $g_s$ ), transpiration rate ( $E$ ), and the abaxial leaf surface temperature with thermocouple ( $T_{abaxial}$ ) were recorded. For the water-use efficiency (WUE) assessment, the intrinsic ( $WUE_{int}$ ;  $P_n/g_s$ ) and instantaneous water-use efficiency ( $WUE_{ins}$ ;  $P_n/E$ ) were estimated [57]. Each measurement was comprised of six replicates with four leaves per replicate. We analysed both control and DTT-infiltrated leaves to evaluate whether DTT used for NPQ assessment influenced leaf gas exchange parameters under constant PAR.

#### 4.7. Models for Fitting of Experimental Data of $T_{leaf}$ and NPQ or $g_s$

Models for fitting experimental data of leaf temperature change ( $\Delta T$ ) and the efficiency of light conversion to heat with qZ component of non-photochemical quenching ( $\Delta NPQ$ ) or stomatal conductance ( $g_s$ ), NPQ induction and gas exchange parameters were performed using OriginPro version 2023b (OriginLab Corporation, Northampton, MA, USA). The models for fitting experimental data were applied as specified for each case and reported with the adjusted  $R^2$  ( $R_a^2$ ) value to determine the goodness of data fitting. We especially applied the following:

- Linear regression fitting model (1) and double logarithmic reciprocal function of Bradley regression model (nonlinear, 2) for fitting data ( $x$ ) of light-induced leaf temperature increase ( $\Delta T$ ) and the efficiency of light conversion to heat with qZ component of non-photochemical quenching ( $\Delta NPQ$ ) at 396  $\mu\text{mol m}^{-2} \text{s}^{-1}$  B (450 nm) light:

$$y = a + b \times x \quad (1)$$

where  $a$  is an intercept and  $b$  is a slope,

$$y = a \times \ln(-b \times \ln(x)) \quad (2)$$

where  $a$  and  $b$  are regression coefficients.

- Allometric model (nonlinear, 3) for fitting data ( $x$ ) of leaf abaxial surface temperature ( $T_{abaxial}$ ) and the stomatal conductance ( $g_s$ ) at 400  $\mu\text{mol m}^{-2} \text{s}^{-1}$  RGB (1:1:1) light:

$$y = a \times x^b \quad (3)$$

where  $a$  is the coefficient of the equation and  $b$  is a power.

- Log-logistic equation with variable Hill slope ( $p$ ) model (nonlinear, 4) for fitting data ( $x$ ) of leaf abaxial surface temperature ( $T_{abaxial}$ ) and the stomatal conductance ( $g_s$ ) at 0–2000  $\mu\text{mol m}^{-2} \text{s}^{-1}$  RB (R:B 10:1) light:

$$y = A_1 + \frac{A_2 - A_1}{1 + 10^{(Log x_0 - x)^p}} \quad (4)$$

where  $A_1$  = bottom asymptote,  $A_2$  = top asymptote,  $Log x_0$  = centre,  $p$  = Hill slope.

Models for fitting gas exchange parameters data against PAR: asymptotic regression model ( $y = a - b \times c^x$ ,  $a$  = asymptote,  $b$  = response range,  $c$  = rate), lognormal cumulative distribution function ( $y = y_0 + A \int_0^x \frac{1}{\sqrt{2\pi} w t} e^{-\frac{(\ln(t) - x_c)^2}{2w^2}} dt$ ,  $y_0$  = offset,  $A$  = amplitude,  $x_c$  = log Mean,  $w$  = Standard Deviation), logistic regression model ( $y = \frac{A_1 - A_2}{1 + (\frac{x}{x_0})^p} + A_2$ ,  $A_1$  = initial value,  $A_2$  = final value,  $x_0$  = centre,  $p$  = power) and sigmoidal model ( $y = \frac{A_1 - A_2}{1 + e^{(x - x_0)/dx}} + A_2$ ,  $A_1$  = initial value,  $A_2$  = final value,  $x_0$  = centre,  $dx$  = constant).

#### 4.8. Statistical Analysis

Statistical analysis was performed using Statistica 13.3 software (StatSoft Inc., Oklahoma, OK, USA). The normal distribution of variables was verified using the Shapiro–Wilk test and the equality of variances was evaluated using Levene's test. One-way ANOVA and post-hoc Tukey's HSD tests were employed to analyse the differences between the investigated groups. The data are presented as mean with standard deviation ( $\pm SD$ ). Statistical significance was determined at the 0.05 level ( $p = 0.05$ ).

### 5. Conclusions

Our results clearly documented that under similar lighting and temperature conditions, the adaxial leaf surface of tomato plants irradiated with moderate light intensity (400  $\mu\text{mol m}^{-2} \text{s}^{-1}$ ) presented significantly higher temperature than the non-irradiated abaxial side. Thus, one might conclude that the major factor contributing to adaxial side temperature is irradiation exposition.

However, an exception to this was G plants, presenting similar foliar temperatures on both leaf sides, thus putting into doubt the postulated influence of direct light exposure on foliar temperature. Additionally, we noticed discrepancies among the recorded  $T_{leaf}$  among the plants of the different spectrum which has been revealed under moderate light intensity. We found, that under constant PAR the  $T_{adaxial}$  temperature is the highest for B light-grown plants and the lowest for the G plants. Taking these results into account, we postulated that the crucial factor contributing to observed  $T_{adaxial}$  discrepancies among treatments is the spectrum-related NPQ amplitude characteristic, responsible for uneven dissipation of absorbed excessive energy within the chloroplasts of the upper side of mesophyll cells. The basis of observed NPQ difference among treatments has been previously explained within distinct patterns of PsbS and VDE protein accumulation - increased level in B-grown plants and reduced under monochromatic G or G-enriched RGB mixed spectrum. In this research, we also proved that DTT application that inhibits zeaxanthin-dependent NPQ component lowering significantly its amplitude is also responsible for the concomitant decrease of foliar temperature. In the case of documented in previous studies the influence of stomatal conductance on leaf energy balance we indeed noted the  $g_s$  influences  $T_{abaxial}$ . At the same time, however, such a regulation is restricted within limited stomatal aperture and density, thus under higher light intensities cooling effect tends to fail in  $T_{leaf}$  regulation.

**Author Contributions:** Conceptualization, M.T. and E.S.; formal analysis, M.T. and E.S.; methodology, E.S.; data curation, M.T.; writing—original draft preparation, M.T. and E.S.; writing—review and editing, M.T. and E.S. All authors have read and agreed to the published version of the manuscript.

**Funding:** This research was funded by the Polish Ministry of Science and Higher Education (Grant No. SUPB.RN.23.248, M.T., E.S) and the Polish Agency for Restructuring and Modernisation of Agriculture (Grant No. DDD.6509.00044.2022.13, M.T., E.S.).

**Institutional Review Board Statement:** Not applicable.

**Informed Consent Statement:** Not applicable.

**Data Availability Statement:** Data are available on request due to restrictions, e.g., privacy or ethics. The data presented in this study are available on request from the corresponding author. The data are not publicly available due to the strict management of various data and technical resources within the research teams.

**Conflicts of Interest:** The authors declare no conflict of interest.

## References

1. Iseki, K.; Olaleye, O. A new indicator of leaf stomatal conductance based on thermal imaging for field-grown cowpea. *Plant Prod. Sci.* **2020**, *23*, 136–147. <https://doi.org/10.1080/1343943X.2019.1625273>
2. Gerhards, M.; Rock, G.; Schlerf, M.; Udelhoven, T. Water stress detection in potato plants using leaf temperature, emissivity, and reflectance. *Int. J. Appl. Earth Obs. Geoinf.* **2016**, *53*, 27–39. <https://doi.org/10.1016/j.jag.2016.08.004>
3. Trojak, M.; Skowron, E. Light quality-dependent regulation of non-photochemical quenching in tomato plants. *Biology* **2021**, *10*, 721. <https://doi.org/10.3390/biology10080721>
4. Durand, M.; Stangl, Z.R.; Salmon, Y.; Burgess, A.J.; Murchie, E.H.; Robson, T.M. Sunflecks in the upper canopy: dynamics of light-use efficiency in sun and shade leaves of *Fagus sylvatica*. *New Phytol.* **2022**, *235*, 1365–1378. <https://doi.org/10.1111/nph.18222>
5. Sukhova, E.; Khlopkov, A.; Vodeneev, V.; Sukhov, V. Simulation of a nonphotochemical quenching in plant leaf under different light intensities. *Biochim. Biophys. Acta - Bioenerg.* **2020**, *1861*, 148138. <https://doi.org/10.1016/j.bbabiobio.2019.148138>
6. Chang, C.Y.Y.; Bräutigam, K.; Hüner, N.P.; Ensminger, I. Champions of winter survival: cold acclimation and molecular regulation of cold hardiness in evergreen conifers. *New Phytol.* **2021**, *229*, 675–691. <https://doi.org/10.1111/nph.16904>
7. Omasa, K.; Takayama, K. Simultaneous measurement of stomatal conductance, non-photochemical quenching, and photochemical yield of photosystem II in intact leaves by thermal and chlorophyll fluorescence imaging. *Plant Cell Physiol.* **2003**, *44*, 1290–1300. <https://doi.org/10.1093/pcp/pcg165>
8. Kaňa, R.; Vass, I. Thermoimaging as a tool for studying light-induced heating of leaves: Correlation of heat dissipation with the efficiency of photosystem II photochemistry and non-photochemical quenching. *Environ. Exp. Bot.* **2008**, *64*, 90–96. <https://doi.org/10.1016/j.envexpbot.2008.02.006>

9. Alonso, L.; Van Wittenberghe, S.; Amorós-López, J.; Vila-Francés, J.; Gómez-Chova, L.; Moreno, J. Diurnal cycle relationships between passive fluorescence, PRI and NPQ of vegetation in a controlled stress experiment. *Remote Sens.* **2017**, *9*, 770. <https://doi.org/10.3390/rs9080770>
10. Kang, H.X.; Zhu, X.G.; Yamori, W.; Tang, Y.H. Concurrent increases in leaf temperature with light accelerate photosynthetic induction in tropical tree seedlings. *Front. Plant Sci.* **2020**, *11*, 1216. <https://doi.org/10.3389/fpls.2020.01216>
11. Kulasek, M.; Bernacki, M.J.; Ciszak, K.; Witon, D.; Karpiński, S. Contribution of PsbS function and stomatal conductance to foliar temperature in higher plants. *Plant Cell Physiol.* **2016**, *57*, 1495–1509. <https://doi.org/10.1093/pcp/pcw083>
12. Trojak, M.; Skowron, E.; Sobala, T.; Kocurek, M.; Pałyga, J. Effects of partial replacement of red by green light in the growth spectrum on photomorphogenesis and photosynthesis in tomato plants. *Photosynth. Res.* **2022**, *151*, 295–312. <https://doi.org/10.1007/s11120-021-00879-3>
13. Urban, J.; Ingwers, M.; McGuire, M.A.; Teskey, R.O. Stomatal conductance increases with rising temperature. *Plant Signal. Behav.* **2017**, *12*, e1356534. <https://doi.org/10.1080/15592324.2017.1356534>
14. Yousef, A.F.; Ali, M.M.; Rizwan, H.M.; Ahmed, M.A.; Ali, W.M.; Kalaji, H.M.; Elsheery, N.; Wróbel, J.; Xu, Y.; Chen, F. Effects of light spectrum on morpho-physiological traits of grafted tomato seedlings. *PLoS One* **2021**, *16*, e0250210. <https://doi.org/10.1371/journal.pone.0250210>
15. Ziegler-Jöns, A.; Knoppik, D.; Selinger, H. The calibration of thermocouples for leaf temperature measurements in gas exchange cuvettes. *Oecologia* **1986**, *68*, 611–614. <https://doi.org/10.1007/BF00378780>
16. Chaerle, L.; Leinonen, I.; Jones, H.G.; Van Der Straeten, D. Monitoring and screening plant populations with combined thermal and chlorophyll fluorescence imaging. *J. Exp. Bot.* **2007**, *58*, 773–784. <https://doi.org/10.1093/jxb/erl257>
17. Welc, R.; Luchowski, R.; Kluczyk, D.; Zubik-Duda, M.; Grudzinski, W.; Maksim, M.; Reszczynska, E.; Sowinski, K.; Mazur, R.; Nosalewicz, A.; Gruszecki, W.I. Mechanisms shaping the synergism of zeaxanthin and PsbS in photoprotective energy dissipation in the photosynthetic apparatus of plants. *Plant J.* **2021**, *107*, 418–433. <https://doi.org/10.1111/tpj.15297>
18. Demmig-Adams, B.; Winter, K.; Kruger, A.; Czygan, F.C. Zeaxanthin and the induction and relaxation kinetics of the dissipation of excess excitation energy in leaves in 2% O<sub>2</sub>, 0% CO<sub>2</sub>. *Plant Physiol.* **1989**, *90*, 887–893. <https://doi.org/10.1104/pp.90.3.887>
19. Demmig-Adams, B.; Adams III, W.W.; Heber, U.; Neimanis, S.; Winter, K.; Krüger, A.; Czygan, F.C.; Bilger, W.; Björkman, O. Inhibition of zeaxanthin formation and of rapid changes in radiationless energy dissipation by dithiothreitol in spinach leaves and chloroplasts. *Plant Physiol.* **1990**, *92*, 293–301. <https://doi.org/10.1104/pp.92.2.293>
20. Srivastava, A.; Zeiger, E. The inhibitor of zeaxanthin formation, dithiothreitol, inhibits blue-light-stimulated stomatal opening in *Vicia faba*. *Planta* **1995**, *196*, 450–457. <https://doi.org/10.1007/BF00203642>
21. Murchie, E.H.; Lawson, T. Chlorophyll fluorescence analysis: a guide to good practice and understanding some new applications. *J. Exp. Bot.* **2013**, *64*, 3983–3998. <https://doi.org/10.1093/jxb/ert208>
22. Hatfield, J.L.; Dold, C. Water-use efficiency: advances and challenges in a changing climate. *Front. Plant Sci.* **2019**, *10*, 103. <https://doi.org/10.3389/fpls.2019.00103>
23. Hamdani, S.; Khan, N.; Perveen, S.; Qu, M.; Jiang, J.; Govindjee; Zhu, X.G. Changes in the photosynthesis properties and photoprotection capacity in rice (*Oryza sativa*) grown under red, blue, or white light. *Photosynth. Res.* **2019**, *139*, 107–121. <https://doi.org/10.1007/s11120-018-0589-6>
24. Yang, Y.N.; Le, T.T.L.; Hwang, J.H.; Zulfugarov, I.S.; Kim, E.H.; Kim, H.U.; Jeon, J.S.; Lee, D.H.; Lee, C.H. High Light Acclimation Mechanisms Deficient in a PsbS-Knockout *Arabidopsis* Mutant. *Int. J. Mol. Sci.* **2022**, *23*, 2695. <https://doi.org/10.3390/ijms23052695>
25. Kim, H.H.; Goins, G.D.; Wheeler, R.M. Stomatal conductance of lettuce grown under or exposed to different light qualities. *Ann. Bot.* **2004**, *94*, 691–697. <https://doi.org/10.1093/aob/mch192>
26. Savvides, A.; Fanourakis, D.; van Ieperen, W. Co-ordination of hydraulic and stomatal conductances across light qualities in cucumber leaves. *J. Exp. Bot.* **2012**, *63*, 1135–1143. <https://doi.org/10.1093/jxb/err348>
27. Lim, S.; Kim, J. Light Quality Affects Water Use of Sweet Basil by Changing Its Stomatal Development. *Agronomy* **2021**, *11*, 303. <https://doi.org/10.3390/agronomy11020303>
28. Li, X.; Zhao, S.; Lin, A.; Yang, Y.; Zhang, G.; Xu, P.; Wu, Y.; Yang, Z. Effect of Different Ratios of Red and Blue Light on Maximum Stomatal Conductance and Response Rate of Cucumber Seedling Leaves. *Agronomy* **2023**, *13*, 1941. <https://doi.org/10.3390/agronomy13071941>
29. Orzechowska, A.; Trtílek, M.; Tokarz, K.M.; Szymańska, R.; Niewiadomska, E.; Rozpądek, P.; Wątor, K. Thermal analysis of stomatal response under salinity and high light. *Int. J. Mol. Sci.* **2021**, *22*, 4663. <https://doi.org/10.3390/ijms22094663>
30. Pérez-Bueno, M.L.; Illescas-Miranda, J.; Martín-Forero, A.F.; de Marcos, A.; Barón, M.; Fenoll, C.; Mena, M. An extremely low stomatal density mutant overcomes cooling limitations at supra-optimal temperature by adjusting stomatal size and leaf thickness. *Front. Plant Sci.* **2022**, *13*, 919299. <https://doi.org/10.3389/fpls.2022.919299>

31. Li, Y.; Xin, G.; Liu, C.; Shi, Q.; Yang, F.; Wei, M. Effects of red and blue light on leaf anatomy, CO<sub>2</sub> assimilation and the photosynthetic electron transport capacity of sweet pepper (*Capsicum annuum* L.) seedlings. *BMC Plant Biol.* **2020**, *20*, 1–16. <https://doi.org/10.1186/s12870-020-02523-z>
32. Chen, L.L.; Wang, H.Y.; Gong, X.C.; Zeng, Z.H.; Xue, X.Z.; Hu, Y.G. Transcriptome analysis reveals effects of red and blue light-emitting diodes (LEDs) on the growth, chlorophyll fluorescence and endogenous plant hormones of potato (*Solanum tuberosum* L.) plantlets cultured in vitro. *J. Integr. Agric.* **2021**, *20*, 2914–2931. [https://doi.org/10.1016/S2095-3119\(20\)63393-7](https://doi.org/10.1016/S2095-3119(20)63393-7)
33. Nie, W.F.; Li, Y.; Chen, Y.; Zhou, Y.; Yu, T.; Zhou, Y.; Yang, Y. Spectral light quality regulates the morphogenesis, architecture, and flowering in pepper (*Capsicum annuum* L.). *J. Photochem. Photobiol. B, Biol.* **2023**, *241*, 112673. <https://doi.org/10.1016/j.jphotobiol.2023.112673>
34. Su, P.; Ding, S.; Wang, D.; Kan, W.; Yuan, M.; Chen, X.; Tang, C.; Hou, J.; Wu, L. Plant morphology, secondary metabolites and chlorophyll fluorescence of *Artemisia argyi* under different LED environments. *Photosynth. Res.* **2023**, 1–12. <https://doi.org/10.1007/s11120-023-01026-w>
35. Kaiser, E.; Ouzounis, T.; Giday, H.; Schipper, R.; Heuvelink, E.; Marcelis, L.F. Adding blue to red supplemental light increases biomass and yield of greenhouse-grown tomatoes, but only to an optimum. *Front. Plant Sci.* **2019**, *9*, 2002. <https://doi.org/10.3389/fpls.2018.02002>
36. Jiang, C.D.; Gao, H.Y.; Zou, Q.; Jiang, G.M. Inhibition of photosynthesis by shift in the balance of excitation energy distribution between photosystems in dithiothreitol treated soybean leaves. *Photosynthetica* **2004**, *42*, 409–415. <https://doi.org/10.1023/B:PHOT.0000046160.18482.91>
37. Ferroni, L.; Colpo, A.; Baldisserotto, C.; Pancaldi, S. In an ancient vascular plant the intermediate relaxing component of NPQ depends on a reduced stroma: Evidence from dithiothreitol treatment. *J. Photochem. Photobiol. B, Biol.* **2021**, *215*, 112114. <https://doi.org/10.1016/j.jphotobiol.2020.112114>
38. Laisk, A.; Oja, V.; Eichelmann, H.; Dall’Osto, L. Action spectra of photosystems II and I and quantum yield of photosynthesis in leaves in State 1. *Biochim. Biophys. Acta - Bioenerg.* **2014**, *1837*, 315–325. <https://doi.org/10.1016/j.bbabiobio.2013.12.001>
39. Wientjes, E.; van Amerongen, H.; Croce, R. LHCII is an antenna of both photosystems after long-term acclimation. *Biochim. Biophys. Acta - Bioenerg.* **2013**, *1827*, 420–426. <https://doi.org/10.1016/j.bbabiobio.2012.12.009>
40. Materová, Z.; Sobotka, R.; Zdvíhalová, B.; Oravec, M.; Nezval, J.; Karlický, V.; Vrábl, D.; Štroch, M.; Špunda, V. Monochromatic green light induces an aberrant accumulation of geranylgeranylated chlorophylls in plants. *Plant Physiol. Biochem.* **2017**, *116*, 48–56. <https://doi.org/10.1016/j.plaphy.2017.05.002>
41. Nelson, J. A.; Bugbee, B. Analysis of environmental effects on leaf temperature under sunlight, high pressure sodium and light emitting diodes. *PloS One* **2015**, *10*, e0138930. <https://doi.org/10.1371/journal.pone.0138930>
42. Kume, A. Importance of the green color, absorption gradient, and spectral absorption of chloroplasts for the radiative energy balance of leaves. *J. Plant Res.* **2017**, *130*, 501–514. <https://doi.org/10.1007/s10265-017-0910-z>
43. Liu, J.; Van Iersel, M.W. Photosynthetic physiology of blue, green, and red light: Light intensity effects and underlying mechanisms. *Front. Plant Sci.* **2021**, *12*, 328. <https://doi.org/10.3389/fpls.2021.619987>
44. Holzwarth, A.R.; Miloslavina, Y.; Nilkens, M.; Jahns, P. Identification of two quenching sites active in the regulation of photosynthetic light-harvesting studied by time-resolved fluorescence. *Chem. Phys. Lett.* **2009**, *483*, 262–267. <https://doi.org/10.1016/j.cplett.2009.10.085>
45. Nilkens, M.; Kress, E.; Lambrev, P.; Miloslavina, Y.; Müller, M.; Holzwarth, A.R.; Jahns, P. Identification of a slowly inducible zeaxanthin-dependent component of non-photochemical quenching of chlorophyll fluorescence generated under steady-state conditions in *Arabidopsis*. *Biochim. Biophys. Acta - Bioenerg.* **2010**, *1797*, 466–475. <https://doi.org/10.1016/j.bbabiobio.2010.01.001>
46. Ware, M.A.; Belgio, E.; Ruban, A.V. Comparison of the protective effectiveness of NPQ in *Arabidopsis* plants deficient in PsbS protein and zeaxanthin. *J. Exp. Bot.* **2015**, *66*, 1259–1270. <https://doi.org/10.1093/jxb/eru477>
47. Nosalewicz, A.; Okoń, K.; Skorupka, M. Non-Photochemical Quenching under Drought and Fluctuating Light. *Int. J. Mol. Sci.* **2022**, *23*, 5182. <https://doi.org/10.3390/ijms23095182>
48. Henningsen, J.N.; Bahamonde, H.A.; Mühling, K.H.; Fernández, V. Tomato and Pepper Leaf Parts Contribute Differently to the Absorption of Foliar-Applied Potassium Dihydrogen Phosphate. *Plants* **2023**, *12*, 2152. <https://doi.org/10.3390/plants12112152>
49. Bian, Z.; Zhang, X.; Wang, Y.; Lu, C. Improving drought tolerance by altering the photosynthetic rate and stomatal aperture via green light in tomato (*Solanum lycopersicum* L.) seedlings under drought conditions. *Environ. Exp. Bot.* **2019**, *167*, 103844. <https://doi.org/10.1016/j.envexpbot.2019.103844>
50. Busch, B.L.; Schmitz, G.; Rossmann, S.; Piron, F.; Ding, J.; Bendahmane, A.; Theres, K. Shoot branching and leaf dissection in tomatoes are regulated by homologous gene modules. *Plant Cell* **2011**, *23*, 3595–3609. <https://doi.org/10.1105/tpc.111.087981>

51. Pinnola, A.; Dall'Osto, L.; Gerotto, C.; Morosinotto, T.; Bassi, R.; Alboresi, A. Zeaxanthin binds to light-harvesting complex stress-related protein to enhance nonphotochemical quenching in *Physcomitrella patens*. *Plant Cell* **2013**, *25*, 3519–3534. <https://doi.org/10.1105/tpc.113.114538>
52. Kalituhu, L.; Beran, K.C.; Jahns, P. The transiently generated nonphotochemical quenching of excitation energy in *Arabidopsis* leaves is modulated by zeaxanthin. *Plant Physiol.* **2007**, *143*, 1861–1870. <https://doi.org/10.1104/pp.106.095562>
53. Herlory, O.; Richard, P.; Blanchard, G.F. Methodology of light response curves: application of chlorophyll fluorescence to microphytobenthic biofilms. *Mar. Biol.* **2007**, *153*, 91–101. <https://doi.org/10.1007/s00227-007-0787-9>
54. Kramer, D.M.; Johnson, G.; Kuirats, O.; Edwards, G.E. New fluorescence parameters for the determination of QA redox state and excitation energy fluxes. *Photosynth. Res.* **2004**, *79*, 209–218. <https://doi.org/10.1023/B:PRES.0000015391.99477.0d>
55. Wang, F.F.; Lian, H.L.; Kang, C.Y.; Yang, H.Q. Phytochrome B is involved in mediating red light-induced stomatal opening in *Arabidopsis thaliana*. *Mol. Plant* **2010**, *3*, 246–259. <https://doi.org/10.1093/mp/ssp097>
56. Yi, H.; Rui, Y.; Kandemir, B.; Wang, J.Z.; Anderson, C.T.; Puri, V.M. Mechanical effects of cellulose, xyloglucan, and pectins on stomatal guard cells of *Arabidopsis thaliana*. *Front. Plant Sci.* **2018**, *9*, 1566. <https://doi.org/10.3389/fpls.2018.01566>
57. Medrano, H.; Tomás, M.; Martorell, S.; Flexas, J.; Hernández, E.; Rosselló, J.; Pou, A.; Escalona, J.M.; Bota, J. From leaf to whole-plant water use efficiency (WUE) in complex canopies: Limitations of leaf WUE as a selection target. *Crop J.* **2015**, *3*, 220–228. <https://doi.org/10.1016/j.cj.2015.04.002>

**Disclaimer/Publisher's Note:** The statements, opinions and data contained in all publications are solely those of the individual author(s) and contributor(s) and not of MDPI and/or the editor(s). MDPI and/or the editor(s) disclaim responsibility for any injury to people or property resulting from any ideas, methods, instructions or products referred to in the content.